INFORMATION TO USERS

This manuscript has been reproduced from the microfilm master. UMI films the text directly from the original or copy submitted. Thus, some thesis and dissertation copies are in typewriter face, while others may be from any type of computer printer.

The quality of this reproduction is dependent upon the quality of the copy submitted. Broken or indistinct print, colored or poor quality illustrations and photographs, print bleedthrough, substandard margins, and improper alignment can adversely affect reproduction.

In the unlikely event that the author did not send UMI a complete manuscript and there are missing pages, these will be noted. Also, if unauthorized copyright material had to be removed, a note will indicate the deletion.

Oversize materials (e.g., maps, drawings, charts) are reproduced by sectioning the original, beginning at the upper left-hand corner and continuing from left to right in equal sections with small overlaps.

Photographs included in the original manuscript have been reproduced xerographically in this copy. Higher quality 6" x 9" black and white photographic prints are available for any photographs or illustrations appearing in this copy for an additional charge. Contact UMI directly to order.

ProQuest Information and Learning
300 North Zeeb Road, Ann Arbor, MI 48106-1346 USA
800-521-0600

LINEWIDTH ENHANCEMENT FACTORS OF SHORT EXTERNAL CAVITY SEMICONDUCTOR LASERS

By

AN HOANG NGUYEN, B.Sc., M.Sc.

A Thesis

Submitted to the School of Graduate Studies

in Partial Fulfilment of the Requirements

for the Degree

Doctor of Philosophy

McMaster University

LINEWIDTH ENHANCEMENT FACTORS OF SHORT EXTERNAL CAVITY SEMICONDUCTOR LASERS

DOCTOR OF PHILOSOPHY McMASTER UNIVERSITY

(Engineering Physics) Hamilton, Ontario

TITLE: Linewidth Enhancement Factors of Short External Cavity Semiconductor Lasers

AUTHOR: An H. Nguyen, B.Sc. (University of Toronto)

M.Sc (University of Toronto)

SUPERVISOR: Professor D. T. Cassidy

NUMBER OF PAGES: xii, 77.

ABSTRACT

This thesis describes the development of a method for measuring the tuning of the emission frequency of semiconductor lasers. This method employs a short external cavity (SXC) mirror, as an external optical feedback element, to alter the resonant condition of the lasers.

The experimental system, which includes an SXC laser module constructed out of a flexure mount concept, was derived from this method. The system was used to make measurements of the frequency tuning of InGaAsP multi-quantum well lasers. Linewidth enhancement factors of these lasers were calculated from the experimental data. It was found that the linewidth enhancement factors of these lasers depend on the wavelengths of emission and are fairly independent of the output powers. It was also found that the linewidth enhancement factors of these lasers decrease as the band gap of the barriers of the quantum wells increases.

ACKNOWLEDGEMENTS

I would like to express my gratitude to my supervisor, Dr. D. T. Cassidy, for his guidance and support throughout the course of this work.

I would like to thank Brian Ventrudo for showing me the way around the lab during the first few months of my studies at McMaster.

I would also like to thank J. F. Hazell who generously supplied the quantum well lasers used in this thesis.

I wish to acknowledge financial support from the Natural Sciences and Engineering Research Council of Canada and the Department of Engineering Physics at McMaster University.

My wife and my son deserve the most thanks of all. Without their love, I would not have been able to see this work to a successful completion.

Finally, special thanks to my parents and my sister for their support and encouragement during the past difficult years.

TABLE OF CONTENTS

LIST OF FIGURES

List of Tables

I- Introduction

The transmission and processing of signals carried by optical beams rather than by electrical currents has been a topic of great interest ever since the early 1960s, when lasers were first developed.

Lasers are devices that generate and amplify coherent radiation at frequencies in the infrared, visible, or ultraviolet region of the electromagnetic spectrum. Lasers emit light in a very narrow wavelength band, and this spectral purity is one of the most important properties of the devices. Although lasers come in a great variety of forms and emit light at widely different frequency ranges, they all consist of the same essential elements. These elements are: (I) a gain medium, through which the electromagnetic radiation can be amplified; (II) a pumping process to excite atoms or molecules of the gain medium into higher energy levels; and, (III) a set of partial feedback elements that allow a beam of radiation to either bounce back into the gain medium or to exit the laser as output. A semiconductor laser is a laser whose gain medium is made of direct band gap semiconductor materials.

Since the beginning, the linewidth and the lineshape of the laser were of great interest. Using thermodynamic properties of optical waveguides and resonant cavities Schawlow and Townes[1] predicted that the linewidth of the laser would narrow inversely

with power and that the line would be Lorentzian in shape. It was later shown by Lax[2] that the treatment by Schawlow and Townes was correct only for lasers operating below threshold. Above threshold, amplitude fluctuations of the laser field are stabilized and this leads to a factor of 2 reduction in the linewidth of the laser.

In the early 1980s when single mode semiconductor lasers operating at room temperature were developed, it was discovered that, unlike gas or solid state lasers and due to their small sizes and low facet reflectivities, the linewidths of semiconductor lasers are broad and readily measured. Fleming and Mooradian[3] made the first careful measurements of the linewidth of semiconductor lasers. They found that the spectral lineshape of semiconductor lasers was indeed Lorentzian and the linewidth decreased inversely with output power of the laser, in agreement with theoretical predictions. They, however, also found the startling fact that the measured linewidth was 50 times greater than that predicted by the corrected Schawlow-Townes formula.

The spectral width of semiconductor lasers is important for several reasons. From the point of view of basic science, the failure of the corrected Schawlow-Townes formula indicates that the physics that underlies the operation of this type of laser was not fully understood, and a better or more complete description of this device is obviously desired. From a practical aspect of the matter, since its inception, the semiconductor laser has been developed from a laboratory curiosity into a reliable and marketable product. It has gained widespread acceptance as a source of light in many varied applications. Due to its small size, its stable operation and the relative ease of modulation, the semiconductor laser is used as a practical light source in optical

communication[4] and in laser spectroscopy[5]. Both of these applications require lasers with narrow spectral width. Motivated by these demands, there has been a flurry of activities, both on the theoretical side to understand the factor that broadens the spectral width of the laser and on the experimental side to measure this elusive quantity[6 7 8 9].

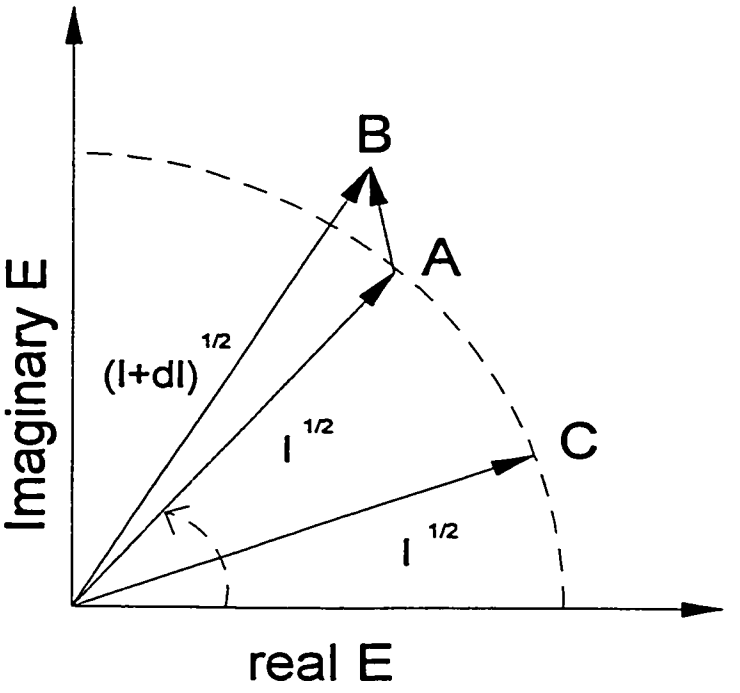

Figure 1: Phasor representation of electric field in a semiconductor laser. Point A represents the laser field before the spontaneous emission event takes place. Immediately after the spontaneous emission, the field sums to point B. After the effect of the gain clamping mechanism, the field returns to steady state at point C.

A couple of years after the experiment of Fleming and Mooradian in 1982, Henry proposed an explanation for the observed linewidth-broadening phenomenon[10]. His explanation is best understood through the phasor model shown in figure 1. In this model, the optical field E of the semiconductor laser is represented by a phasor of length $\sqrt{I}$, where I is the intensity of the lasing mode. This phasor rotates in the complex plane at the oscillation frequency ω. Fluctuations in the optical field due to spontaneous emission are accounted for by the addition of vectors with length unity and random phase to the end of the field phasor. Such events cause changes in both the length of the phasor (field amplitude) and its phase. Besides the instantaneous phase change caused by spontaneous emission, there will be a delayed phase change accumulated as the laser undergoes relaxation oscillation to slowly return to the steady state field intensity. During this time there will be a net gain change proportional to $\Delta n''$, the deviation of the imaginary part of the refractive index from its steady state value. This change in n'', caused by a change in carrier density, will also alter the real part of the refractive index n'. The ratio of these changes is $\alpha = \Delta n' / \Delta n''$.

Using Langevin's rate equations with driving terms for the field amplitude and for the carrier density of the laser, Henry managed to derive a new formula for the linewidth of the semiconductor laser. Similar to the Schawlow-Townes formula, the linewidth predicted by Henry narrows inversely with the output power of the laser and the spectral lineshape is Lorentzian. Henry's most important contribution is the fact that

his formula also predicts that the linewidth will be broadened by a factor $(1+\alpha^2)$, where α is the ratio of the change of the real part over the change of the imaginary part of the refractive index mentioned earlier. Due to the effect of this quantity on the linewidth of the laser, α is now called the linewidth enhancement factor.

Encouraged by this theoretical breakthrough and by the importance of the linewidth enhancement factor in semiconductor lasers, a large number of experimental techniques[11 12 13 14 15] were soon developed to measure this quantity and to study the effect it has on the operation of the laser. Among these techniques, the most popular ones are : (I) the small signal modulation technique[14 15]; (II) the method of spontaneous emission measurement [8 16]; and, (III) the method of optical injection locking[12 17]. In the small signal modulation technique, the tested laser is DC biased and modulated at frequencies in the order of GHz, over a wide range of frequencies. This is usually done with a network analyzer. From the light output of the modulated laser both frequency modulation and amplitude modulation indices are obtained. The ratio of these two indices is related to the linewidth enhancement factor α by an equation, which also contains the damping rate of the laser and the modulation frequency. Although this method can be used to measure simultaneously the linewidth enhancement factor, the AM and FM response, and the damping rate of semiconductor lasers, the method requires high frequency modulation of the injection current and the dynamic instability of the laser system may interfere with measurements. Furthermore, there are inherent difficulties in high-speed measurement techniques such as impedance matching between various parts of the experimental set up, and signal attenuation at high frequencies. In the

method of spontaneous emission measurement, first developed by Henry and coworkers[18], the spontaneous emission spectra of a semiconductor laser operating under threshold is recorded. From this data the optical gain profile is extracted. The key to determining the optical gain from the spontaneous emission spectrum is the knowledge of the quasi-Fermi level separation ΔE_F and a scaling constant, which allows the passage from a spectrum to modal gain. This data often is extracted by fitting the measured curves to a theoretical model[19 20]. Aside from the question of how sophisticated such a model should be, this raises the problem of the parameters used in the model, as they are frequently obtained from measurements on other devices. Furthermore, using this technique, the refractive index profile has to be obtained separately, either by a Kramers-Kronig relation from the fitted gain profile or by some different method. The linewidth enhancement factor, when finally derived from these two profiles contains a dubious level of accuracy. This measurement method for the linewidth enhancement factor is certainly not straightforward, and some interesting information such as the dependence of the linewidth enhancement factor on the output of the laser is not readily available. Finally, in the method of optical injection locking, a laser oscillator (a slave laser) is synchronized to another stable laser oscillator (a master laser). The locking bandwidth of this system is found to become asymmetric when the linewidth enhancement factor $\alpha \neq 0$ and the value of α can be evaluated from this asymmetry. In this kind of method at least two lasers are required and the accuracy of the measurement is affected by the frequency stability of both lasers[12].

This thesis describes the development of a method for measuring the linewidth enhancement factor of a wide range of semiconductor lasers. This method overcomes a number of limitations discussed earlier and provides additional information about the laser. Based on a theoretical study of short external cavity lasers, an experimental method is presented to measure the linewidth enhancement factor of semiconductor lasers. In this method, by changing the length of the short external cavity the resonant condition of the semiconductor laser is altered. This new resonant condition leads to a shift in the emission frequency, which can be used to deduce the linewidth enhancement factor of the laser. The experimental method can be used to investigate the connection between the linewidth enhancement factor of the laser and many of its intrinsic properties such as spectral width, FM noise, and correlation between AM and FM noise. As a demonstration of the developed method, the experimental system was first used to measure the linewidth enhancement factors of a quantum well laser and an index-guided laser with bulk active region (or index-guided laser for short). Independent measurements of linewidths were performed for these two lasers. The correlation between this data and the linewidth enhancement factors are presented as confirmation for the validity of the newly developed method. The experimental system was then used to measure the linewidth enhancement factors of five different InGaAsP multi-quantum well lasers. The dependence of the linewidth enhancement factor on the output power, on the wavelength of emission and on the heights of the barriers of the quantum wells are investigated.

A significant portion of the work reported in this thesis was devoted to the design of a flexure mount; a device that could be used to force multi-mode Fabry-Perot semiconductor lasers into single mode oscillations.

There were several motivations for this study. Very few physical processes affect the performance of semiconductor lasers more significantly than the coupling between the phase and the intensity of the optical field in a laser cavity. Therefore, a better understanding of the nature and the influence of the linewidth enhancement factor not only provides better insights into the physics of the laser but also goes a long way in assisting the design of lasers with better performance. Short external cavity (SXC) lasers have been used within this research group at McMaster for spectroscopy[21] and as a means for studying laser device physics. The developed method of measuring the linewidth enhancement factor will augment the SXC laser technology as a research tool.

The thesis is structured as follows: In chapter 2, the model of a short external cavity (SXC) semiconductor laser with an external mirror employed as the feedback element is described. By following the light-wave as it traverses around both the laser and the external cavity how the presence of this short external cavity (SXC), formed by the mirror and the rear facet of the laser, alters the output characteristics of the laser is shown. It is also shown that by slightly altering the length of this external cavity, the emission frequency of the laser is shifted and a master equation that relates this frequency shift to the linewidth enhancement factor α is derived. In chapter 3, the first part is devoted to a description of the design and the performance of the flexure mount. This device was originally intended for use in this work, but other applications have been

found for it as well. In the later part of this chapter, a description of an experimental set-up to measure the change in the emission frequency of the laser, as the position of the external cavity mirror is made to vary, is given. This set-up is a realization of the model developed in chapter 2. In chapter 4, measurements on two lasers, an index-guided laser with a bulk active region and a multi-quantum well laser, are reported. Frequency shift measurements for each of these lasers were done on the six longitudinal modes for which single-frequency operation could be obtained. In this chapter, the method employed to fit the collected data to the master equation so that the corresponding α factors could be deduced is also explained. Finally, to demonstrate the validity of this method, independent linewidth measurements were done on these lasers and the correlation between these linewidths and the linewidth enhancement factors is presented. In chapter 5, the data of measurements of the linewidth enhancement factors performed on five InGaAsP multi-quantum well lasers are presented. This data reveals the dependence of the linewidth enhancement factors on various laser parameters, such as output power, wavelength of emission and heights of the quantum-well barriers. In the conclusion, which makes up chapter 6, a summary of the work done in this thesis is given. The difficulties inherent in the developed method and various possible improvements, along with recommendations for future work are discussed.

II- Theory

This chapter deals with the theory that lays out the foundation for this thesis. In the first section, a qualitative description of semiconductor lasers is given. In the second section, the model of a short external cavity laser is presented. In the third section, the relationship between the tuning of the emission frequency and the linewidth enhancement factor of the semiconductor laser is derived.

II-1 Semiconductor Lasers Background

A diode laser consists of a single crystal of direct band-gap[22] semiconductor material. To date, most laser diodes have been made using $GaAs$, $Ga_{(1-x)}Al_xAs$, or $In_{(1-x)}Ga_xAs_{(1-y)}P_y$, but other materials will no doubt eventually be used to obtain emission at different wavelengths. The most basic structure of the laser diode is a p-n junction[23]. When this p-n junction is forward biased, the holes in the p-type region are injected into the n-type region, while electrons in the n-type are injected into the p-type region. When an electron meets a positive hole, they combine together, emitting a photon of energy nearly equal to the band-gap energy. The region where these activities occur is called the active region. The wavelength of emission of a diode laser depends mainly on the type of semiconductor material that it is made of. However, this lasing wavelength can vary slightly with operating temperature and current of the laser. Furthermore, if the p-n junction is made from a quaternary crystal such as

$In_{(1-x)}Ga_xAs_{(1-y)}P_y$ the diode laser has an emission wavelength which could be set by varying the fraction ratios x and y. A basic structure of a p-n junction laser diode is shown in figure 2.

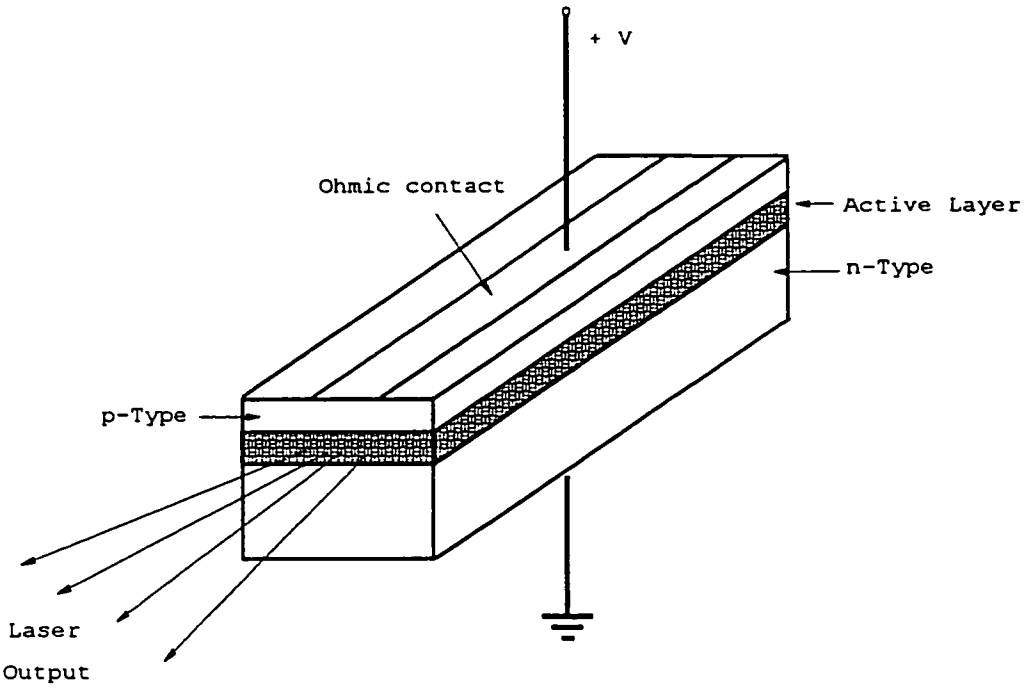

Figure2: Simple semiconductor laser.

The length of a semiconductor laser is normally 200-500 μm. Ohmic contacts are made to both p- and n-regions to permit the flow of electrical current, which is the energy required to produce the inverted population in the active region. The directivity of the output from the semiconductor is not sharp. The output spreads out by as much as 30 degrees. This is because the light is emitted from the active region, a very small area

whose sides are less than 2-3 μm. The intensity of the emitted light is a function of injection current and it is found that this intensity increases rapidly above a certain current I_{th}, while below I_{th} it is rather weak. I_{th} is the starting current for laser oscillation and is called the threshold current. The partially reflecting end faces of the laser diode, formed by cleaving the laser chip along a crystal plane, provide an optical feedback that leads to the establishment of one or more longitudinal modes. Longitudinal modes of the laser are centered at frequencies where a half-integral number of wavelengths equals the length of the optical cavity. Thus, $m\lambda/2 = nL$, where L is the length of the laser, n is the index of refraction of the laser material, and λ is the wavelength of the emitted light. The separations in frequency of these longitudinal modes are given by the free spectral range (FSR) of the laser cavity, $FSR = c/(2n_g L)$, where n_g is the group index of refraction. Normally, a laser will oscillate on a number of these modes. To achieve single mode operation, additional arrangement must be made to suppress all but the preferred mode of the laser. Such a specialized device will be presented in the next chapter.

II-2 Model of Short External Cavity (SXC) Laser

Weak optical feedback, as provided by an external mirror, will alter both the resonant frequency and the intensity of the output of the laser. These changes may serve for the selection of a distinct longitudinal mode of the laser[24], or for tuning of the

emission frequency[25] [26]. To quantify this feedback induced frequency shift, an analysis based on the arrangement shown in Fig. 3 is carried out.

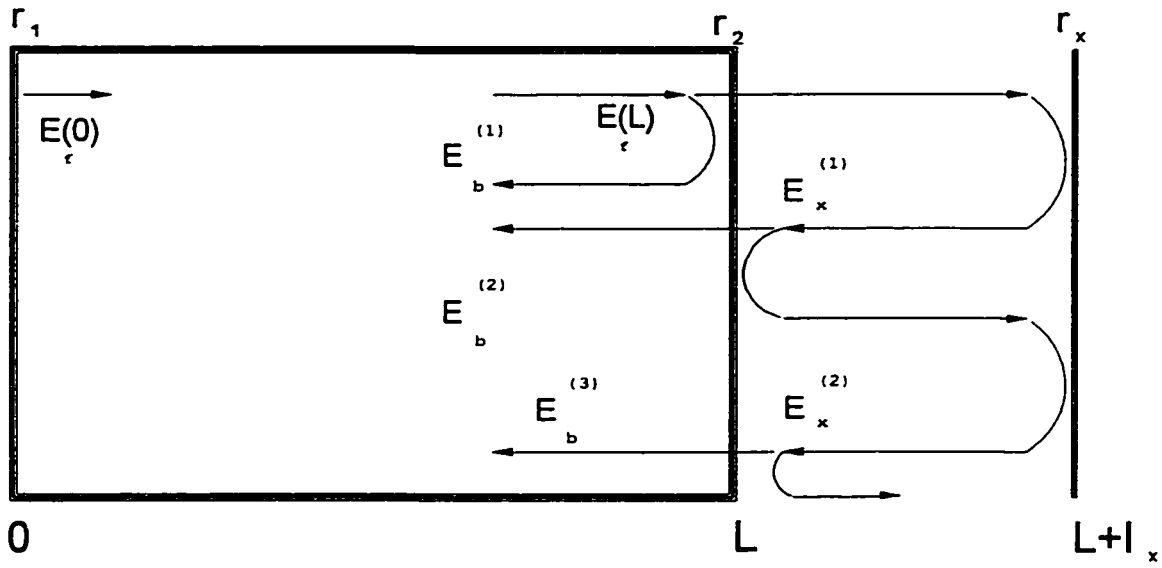

Figure3: Schematic diagram of a semiconductor laser with an external mirror.

The arrangement shown in Fig. 3 consists of a Fabry-Perot laser with facet amplitude reflection coefficients r_1, r_2 and length L. An external mirror is positioned at a distance l_x away from the back facet of the laser to form a short external cavity (SXC). Normally, the length of this SXC is between 160 μm and 200 μm. This external cavity mirror has an amplitude reflection coefficient r_x. The effect of this external mirror on the operation of the SXC laser may be understood by following the light waves as they

propagate inside this compound cavity. To this end, assume that the laser oscillates in a single mode, and let the electric field traveling from the front facet to the back facet of the laser be E_f and the electric field traveling in the opposite direction be E_b. Furthermore, at the front facet $E_f = E_f(0)$ and $E_b = E_b(0)$. Similarly, at the back facet of the laser $E_f = E_f(L)$ and $E_b = E_b(L)$.

The steady state operation of the laser can be described, if one neglects the spontaneous emission, by the following set of equations:

$$E_f(L) = E_f(0)e^{\left(\frac{gL}{2} - jkL\right)} \tag{1}$$

$$E_b(L) = E_b^{(1)} + E_b^{(2)} + E_b^{(3)} + E_b^{(4)} + ... \tag{2}$$

$$E_b(0) = E_b(L)e^{\left(\frac{gL}{2} - jkL\right)} \tag{3}$$

and

$$E_f(0) = r_1 E_b(0). \tag{4}$$

Here, exp(gL/2) is the net single-pass gain through the cavity of the laser, and $k = 2\pi/\lambda$ is the wave vector. In Eq. (2), $E_b^{(1)} = r_2 E_f(L)$ is the reflected wave inside the cavity of the laser while $E_b^{(2)}, E_b^{(3)}, E_b^{(4)} \ldots$ are waves that re-entered the cavity after one, two, three, ... round trips inside the SXC. These feedback fields can be written explicitly as follows:

$$E_b^{(2)} = \sqrt{C} t_2 t_2' r_x e^{(-j\delta)} E_f(L).$$

$$E_b^{(3)} = C t_2 t_2' r_x^2 (r_2') e^{(-j2\delta)} E_f(L).$$

$$E_b^{(4)} = C^{\frac{3}{2}} t_2 t_2' r_x^3 (r_2')^2 e^{(-j3\delta)} E_f(L).$$

Or more generally,

$$E_b^{(n)} = C^{\frac{(n-1)}{2}} t_2 t_2' r_x^{(n-1)} (r_2')^{(n-2)} e^{[-j(n-1)\delta]} E_f(L) \qquad n = 2, 3, 4, \ldots$$

with $t_2 t_2' = 1 - r_2^2$ and $r_2' = -r_2$.

Note that in these equations, $\delta = 2k_0 l_x$ is the phase collected by the electric field after each round trip in the SXC. The factor $r_x\sqrt{C}$ represents the fraction of light that is coupled back into the cavity of the laser after each round trip in the SXC. The magnitude of this factor depends on both the reflectivity and the alignment of the external mirror. Bonnel and Cassidy[27] presented an explicit form for $r_x\sqrt{C}$, which includes both the angular orientation $\kappa(\theta,\varphi)$ of the external mirror with respect to the optical axis of the laser and the length l_x of the short external cavity. In their paper, the level of optical feedback is found by calculating the coupling efficiency between the output beam at the laser facet and the evolved reflected beam. In the calculation presented here the distance l_x is kept explicitly as an independent variable while the effect of the angular orientation of the mirror of the short external cavity is estimated through a fitting parameter.

From here on, for brevity we define $\xi = r_x\sqrt{C}$.

Explicitly,

$$\xi = r_x\sqrt{C} = r_x\sqrt{\frac{\omega_0^2}{\omega_x^2}\exp(-\frac{2k^2 l_x^2\omega_0^2}{\omega_x^2})\kappa(\theta,\varphi)}\,. \tag{5}$$

Here $2\omega_0$ is the beam waist at the facet of the laser and $2\omega_x$ is the beam diameter[28] of the reflected beam.

From Eq. (2)

$$E_b(L) = r_2 E_f(L) + \xi\ t_2\ t_2' e^{(-j\delta)} E_f(L) + \xi^2 t_2\ t_2'(r_2') e^{-j2\delta} E_f(L) + \xi^3 t_2\ t_2'(r_2')^2 e^{-j3\delta} E_f(L) + \ldots$$

With $t_2\ t_2' = 1 - r_2^2$ and $r_2 = -r_2'$ the above equation can be written as

$$E_b(L) = r_2 E_f(L) + \left[\left(1 - r_2^{\,2}\right)\left(\xi\ e^{-j\delta}\right)\sum_{n=1}^{\infty}\left(\xi\ (-r_2) e^{-j\delta}\right)^{n-1}\right] E_f(L)\,.$$

Since in our experiment:

$$\left|\xi(-r_2)e^{-j\delta}\right| << 1 \qquad \text{(weak feed back)}$$

(The typical magnitude of this coupling factor in our experiment is about 10^{-3})

$$E_b(L) = \left[r_2 + \frac{\left(1 - r_2^{\,2}\right)\left(\xi\ e^{-j\delta}\right)}{1 + \xi\ r_2 e^{-j\delta}}\right] E_f(L) \equiv r(\nu) E_f(L) \tag{6}$$

where

$$r(\nu) = r_2 + \frac{\left(1 - r_2^{\,2}\right)\left(\xi\ e^{-j\delta}\right)}{1 + \xi\ r_2 e^{-j\delta}}\,. \tag{7}$$

By substituting Eqs. (1), (3) and (6) into Eq. (4) one arrives at

$$r_1 r(\nu) e^{(gL - j2kL)} = 1. \qquad (8)$$

Note that Eq. (8) is the standard requirement[29] for steady state operation of a "solitary" laser with facet reflectivities of r_1 and r(ν) when spontaneous emission is ignored. So, the effect of the SXC mirror on the output of the laser can be modeled by allowing the back facet reflectivity to depend on the intensity, the phase, and the length of the external cavity for a given frequency of the feedback light[30].

II-3 Tuning Property of SXC Laser Frequency

We begin the study of the frequency tuning characteristic in short external cavity lasers by writing:

$$r(\nu) \equiv r_m e^{-j\phi_m} \qquad (9)$$

and by using Eq. (8) we have

$$r_1 r_m e^{(gL - j2kL - j\phi_m)} = 1.$$

This equation can be separated into the usual phase and gain conditions for steady state operation:

$$r_1 r_m e^{gL} = 1 \qquad \text{(gain condition)} \quad (10)$$

$$\phi_L = 2kL + \phi_m = 2m\pi, \text{ m integer} \qquad \text{(phase condition)} \quad (11).$$

Using Eqs. (7) and (9) in Eqs. (10) and (11) we have

$$\phi_m = \tan^{-1}\left[\frac{\xi\left(1-r_2^{\,2}\right)\sin\delta}{r_2+\xi\left(1+r_2^{\,2}\right)\cos\delta+\xi^2 r_2}\right] \tag{12}$$

and

$$r_m = \frac{\left[r_2+2\xi\left[r_2+\left(1+r_2^{\,2}\right)\cos\delta\right]+\xi^2\left[\left(1+r_2^{\,2}\right)^2+2r_2^{\,2}\cos(2\delta)\right]+2\xi^3\left[r_2\left(1+r_2^{\,2}\right)\cos\delta\right]+\xi^4 r_2^{\,2}\right]^{1/2}}{1+2\xi\ r_2\cos\delta+\xi^2 r_2^{\,2}} \tag{13}$$

Note that in these equations, as before, $\delta = 2k_0 l_x = 4\pi l_x/\lambda = 2\pi\nu\tau_x$ is the phase collected by the electric field after each round trip in the SXC, and $\tau_x = 2l_x/c$ is the transit time in the external cavity.

Now, from Eqs. (12) and (13) by taking the limit as either $r_x \to 0$ or $l_x \to \infty$, it can be seen that in the absence of the SXC mirror, $\phi_m = 0$ and $r_m = r_2$. Under this condition Eqs. (10) and (11) reduce to the standard condition for steady state operation of a solitary laser[29]. In the event of feedback, however, both the emission frequency and the threshold gain of the laser change with changes in l_x. These changes lead to the change in the refractive index μ_e. Keeping this in mind, Eq. (11) will be rewritten as follows:

$$\phi_L = \frac{4\pi L\mu_e\nu}{c} + \phi_m = 2m\pi\,. \tag{14}$$

For the laser system to remain in steady state as the length of the SXC is altered slightly the changes discussed above have to be in such a way that the phase condition (11) is satisfied, i.e.,

$$\Delta\phi_L = \frac{4\pi L}{c}\Delta(\mu_e \nu) + \Delta\phi_m = 0. \tag{15}$$

Following Petermann's arguments[30]

$$\Delta\phi_L = \frac{4\pi L}{c}[\nu_{nf}\Delta\mu_e + (\nu - \nu_{nf})\mu_e] + \Delta\phi_m = 0$$

where the subscript nf means no feedback.

Using

$$\Delta\mu_e = \frac{\partial\mu_e}{\partial n}(n - n_{nf}) + \frac{\partial\mu_e}{\partial\nu}(\nu - \nu_{nf})$$

and with n representing the carrier density, we have

$$\Delta\phi_L = \frac{4\pi L}{c}[\{\frac{\partial\mu_e}{\partial n}(n - n_{nf}) + \frac{\partial\mu_e}{\partial\nu}(\nu - \nu_{nf})\}\nu_{nf} + \mu_e(\nu - \nu_{nf})] + \Delta\phi_m = 0 \tag{16}$$

but since

$$\frac{\partial\mu_e}{\partial n} = -\frac{\alpha c}{4\pi\nu_{nf}}\frac{\partial g(n)}{\partial n}$$

and by assuming that the gain varies linearly with the carrier density, i.e.,

$$\frac{\partial g(n)}{\partial n}(n - n_{nf}) = g(n) - g(n_{nf})$$

Eq. (16) becomes

$$\Delta\phi_L = \frac{4\pi L}{c}[\{\frac{-\alpha c}{4\pi\nu_{nf}}(g(n)-g(n_{nf}))+\frac{\partial\mu_e}{\partial\nu}(\nu-\nu_{nf})\}\nu_{nf}$$

$$+\mu_e(\nu-\nu_{nf})]+\Delta\phi_m = 0 \qquad (17)$$

or

$$\Delta\phi_L = -\alpha L[g(n)-g(n_{nf})]+\frac{4\pi L}{c}[\frac{\partial\mu_e}{\partial\nu}\nu_{nf}+\mu_e][\nu-\nu_{nf}]+\Delta\phi_m = 0.$$

Since the group index $\bar{\mu}_e = \frac{\partial\mu_e}{\partial\nu}\nu_{nf}+\mu_e$

$$\Delta\phi_L = -\alpha L[g(n)-g(n_{nf})]+\frac{4\pi L}{c}\bar{\mu}_e[\nu-\nu_{nf}]+\Delta\phi_m = 0. \qquad (18)$$

Now from Eq. (9)

$$g(n)-g(n_{nf}) = -\frac{1}{L}\ln(\frac{r_m}{r_2})$$

where the dependence of g on n has been written explicitly, and $r_2 = r_m$ when there is no feedback.

Using the above expression for $g(n)-g(n_{nf})$ Eq. (18) becomes

$$\Delta\phi_L = \alpha\ln(\frac{r_m}{r_2})+\frac{4\pi L}{c}\bar{\mu}_e[\nu-\nu_{nf}]+\Delta\phi_m = 0. \qquad (19)$$

In the experimental set-up the level of feedback is low enough[31] so we only need to include the light-waves that travel at most two round trips in the SXC before re-entering the cavity of the laser. Using this simplification and Eq. (12) we have:

$$\frac{\partial\phi_m}{\partial\nu} \cong \frac{2\pi\tau_x\xi\{r_2[1-r_2^2]\cos\delta+[1-r_2^4]\xi\}}{\{r_2+[1+r_2^2]\cos\delta\}^2} \qquad (20)$$

and from Eq. (13)

$$\ln(\frac{r_m}{r_2}) \cong \frac{\xi}{r_2^2}\{r_2 + [1 + r_2^2 - 2r_2^3]\cos\delta\} +$$

$$+ \frac{\xi^2}{r_2^4}\{-[r_2^6 + 3r_2^2] + 2r_2[1 + r_2^2]\cos\delta - 4[1 + 2r_2^2 + 3r_2^6]\cos^2\delta\} \qquad (21)$$

From Eq. (19) the frequency shift induced by feedback from the SXC mirror is given as:

$$(\nu - \nu_{nf}) = \frac{-\alpha \ln\{\frac{r_m(\xi,\delta)}{r_2}\}}{\frac{4\pi L}{c}\overline{\mu}_e + \frac{\partial \phi_m(\xi,\delta)}{\partial \nu}} \qquad (22)$$

Eq. (22) is the desired result. It relates the shift of the emission frequency to the linewidth enhancement factor of the laser. The effect of the external cavity is contained in the dependence of r_m and ϕ_m on the coupling factor ξ, which is defined in Eq.5, and the phase $\delta = 4\pi l_x / \lambda = 2\pi\nu\tau_x$. From Eq. (22) it can be seen that by slightly altering the SXC length l_x, which is implicit in δ and ξ, the resulting change in the emission frequency, once measured, can be used to deduce the linewidth enhancement factor α.

II-4 Summary

In this chapter, a description of a semiconductor laser and the effect of a short external cavity on the output of the laser have been given.

From the description of the SXC laser, it was found that by changing the length of the short external cavity one could cause the emission frequency of the laser to shift.

The relationship between the shift in the frequency of emission of the laser and the linewidth enhancement factor was derived.

The construction of the SXC laser module is presented in the next chapter. Also in the next chapter, an experimental method to measure the shift of the emission frequency is presented.

III- Experimental Apparatus and Technique

This chapter describes the experimental apparatus and technique developed for measuring the tuning of the emission frequency as the length of the external cavity of the SXC laser is varied. In the first section, the construction of a short external cavity (SXC) module based on the flexure mount concept[32] is presented. The SXC system is an inexpensive and simple means to achieve single-mode operation from normally multi-mode lasers. In the second section, a description of the optical apparatus and of the electrical equipment of the experimental set-up is given. This section also describes the experimental procedure to measure the shift of the emission frequency.

III-1 The Flexure Mount

In this section, a short external cavity (SXC) module based on the flexure mount concept is described. The module consists of an external mirror clamped on a flexure bracket and a laser fastened firmly to a flexure base[33]. The mirror is used to feed a portion of the light output back into the laser cavity. The result is that the output of a particular laser mode is enhanced at the expense of the other modes[27]. By altering the length of the external cavity, different modes can be selectively enhanced. The SXC system presented here is inexpensive to construct. It is compact, sensitive, stable, and with the use of the flexure mounts, the alignment of the external mirror is straightforward.

The SXC assembly consists of two major components, a mounting bracket and a baseplate. As shown in Fig. 4, each piece is an independent flexure mount, which was made of aluminum. The mounting bracket [Fig. 4(a)] is used to hold a piezoelectric transducer positioner (PZT) (Physik Instrumente model P-171 with tapped end pieces) that drives the external mirror attached to its front plate. The baseplate consists of two layers [Fig. 4(b)]. With the lower surface L fixed, any element affixed to the upper surface U may be rotated in the vertical direction about the xx axis by adjusting the pair of screws located at B.

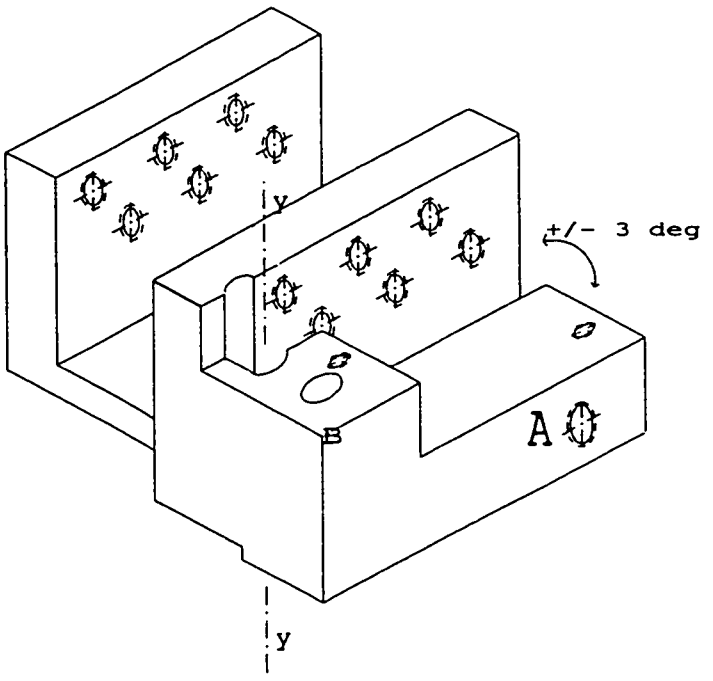

Figure 4(a): Mounting bracket. A and B are precision adjusting screws.

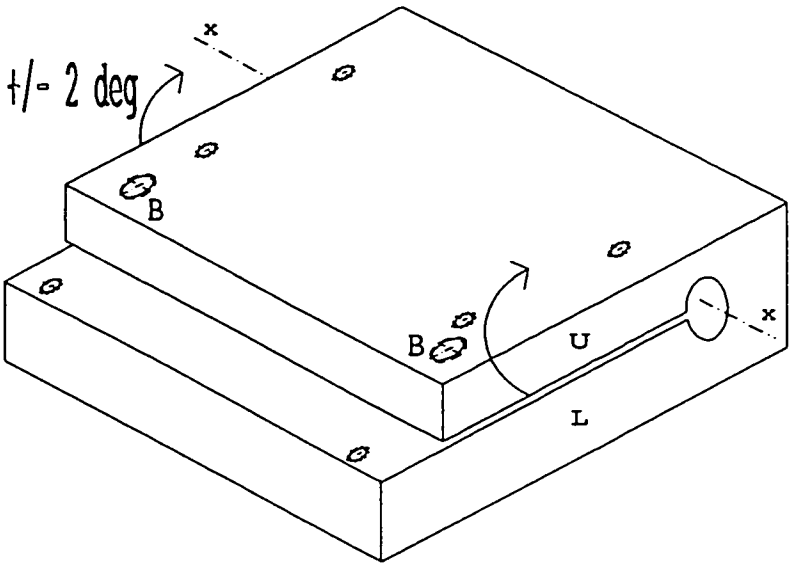

Figure 4(b): Base plate. B's are precision adjusting screws. U and L are upper and lower plates.

The SXC mirrors used in our lab are either gold-coated diamond heat sinks (0.25X0.25X0.40 mm^3) with a polished surface (Dubbledee Diamonds Corporation stock items) or, when higher side mode suppression ratio (SMSR) is required, spherical reflectors formed by impression of a precision ball bearing of 380 μm diam into polished aluminum. The mirror is epoxied to a No. 80 drill bit that is expoxied into a brass washer that is fastened to the front plate of the piezoelectric positioner (Fig. 5). To align the mirror in the horizontal direction, precision adjusting screws are provided through opposite sides of the mounting bracket [see Fig. 4(a)]. When driven against the walls of the mounting channel, these screws (labeled A in the figure) rotate the channel about the yy axis. By using two screws on opposite sides of the channel, adjustment may be made

in either direction from center, and the unused screw may then be used to lock the alignment if desired.

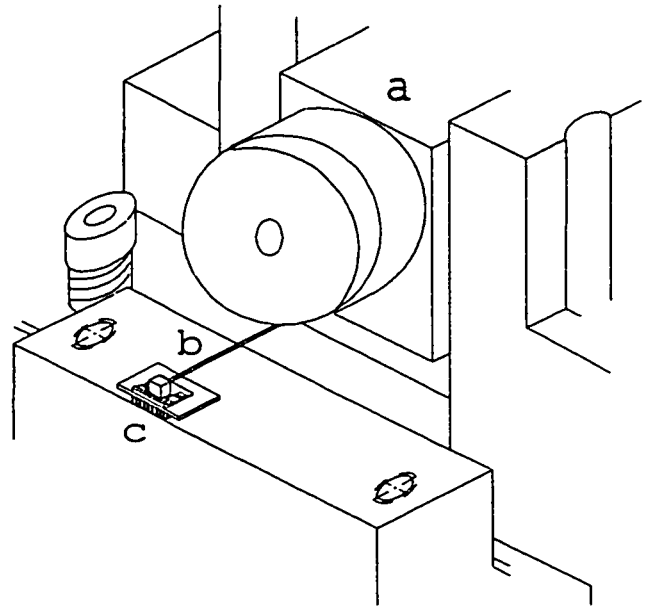

Figure 5: SXC assembly. (a) piezoelectric positioner, (b) No. 80 drill bit which attaches the mirror to the PZT, (c) laser and thermoelectric cooler.

As seen in Fig. 6, the laser is mounted on a separate aluminum block, which is fastened onto the lower surface L, while the mounting bracket is affixed to the upper surface U of the baseplate. This arrangement is necessary to ensure that the mirror is free to rotate while the laser stays in a fixed position, hence the alignment with external optical elements is not affected by the alignment of the external cavity. Together, the mounting bracket and the baseplate form a "two-way" flexure mount which permits ±3°

of rotational alignment in the horizontal direction and ±2° of rotational alignment in the vertical direction for the external cavity mirror.

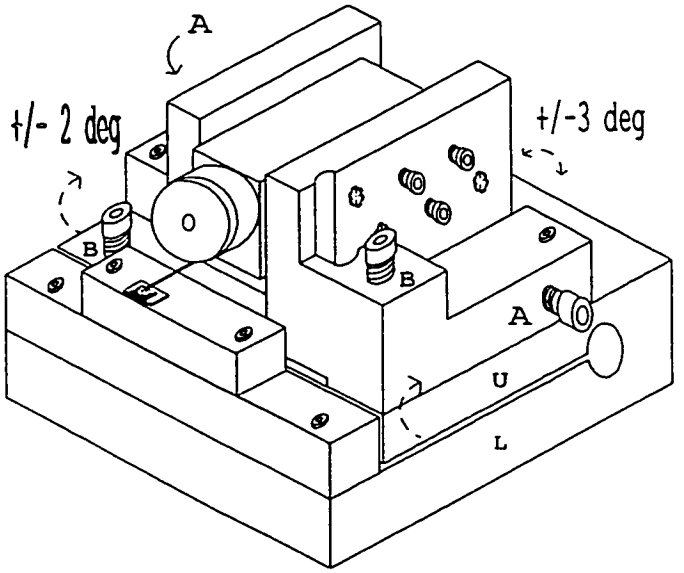

Figure 6: Flexure SXC module. (A) precision screws on both sides for horizontal alignment and (B) precision screws tapped through the upper plate U for vertical alignment.

When a laser is installed in an SXC assembly, the mirror must be aligned to provide optical feedback. The alignment is usually carried out in two steps. In the first step, the end plate of the PZT is attached to an XYZ-translational stage (Newport model 460 XYZ), which has been mounted on a tilt and rotate stage (Newport model 37). The degree of alignment is judged by observing the single-mode power, the side-mode suppression, and the single-mode tuning range of the output of the laser with a scanning monochromator. Once a reasonably good alignment is obtained, i.e., when the external

mirror is positioned in the range of ~100 to ~200 μm behind the facet of the laser diode and a useful side mode suppression ratio is obtained (in the range between 100 and 150), the PZT is clamped into position using the set screws threaded through the walls of the mounting channel. When higher SMSR is required, the mirror needs to be readjusted in such a way that a ray of light travelling down the optical axis of the laser is reflected back down its own path. Using the flexure mount, this very fine adjustment can be accomplished with ease. In this final step, by adjusting the screws labeled A and B in Fig.6 the channel of the mounting bracket in the SXC assembly can be made to rotate both in the vertical and the horizontal directions. This, in turn, causes the same amount of rotational alignment on the mirror with respect to the laser fastened firmly to the lower plate of the base. When the final alignment has been made, i.e., when the planar surface of the mirror and the back facet of the laser are parallel, or, for the case of spherical reflectors, when maximum SMSR is reached, the same set of screws (A and B), which has been pressed firmly against the sides of the mounting channel and the lower plate of the base, clamps the mirror in its final position.

By its nature, the flexure mount is extremely versatile. The actual dimensions depend on a particular application at hand. The amount of spring loading on the adjusting screws A and B can be varied by choice of material and hole spacing. The length of the lever arms from the adjusting screws determines the range of adjustment.

In our application, we found that when using aluminum, the baseplate should be at least 0.9 inches thick so that the module is not sensitive to external mechanical vibration. Also, the lower plate L should be substantially thicker than the upper plate U.

This is to ensure that the laser fastened to the lower plate remains stationary while the mounting bracket attached to the upper plate flexes upwards.

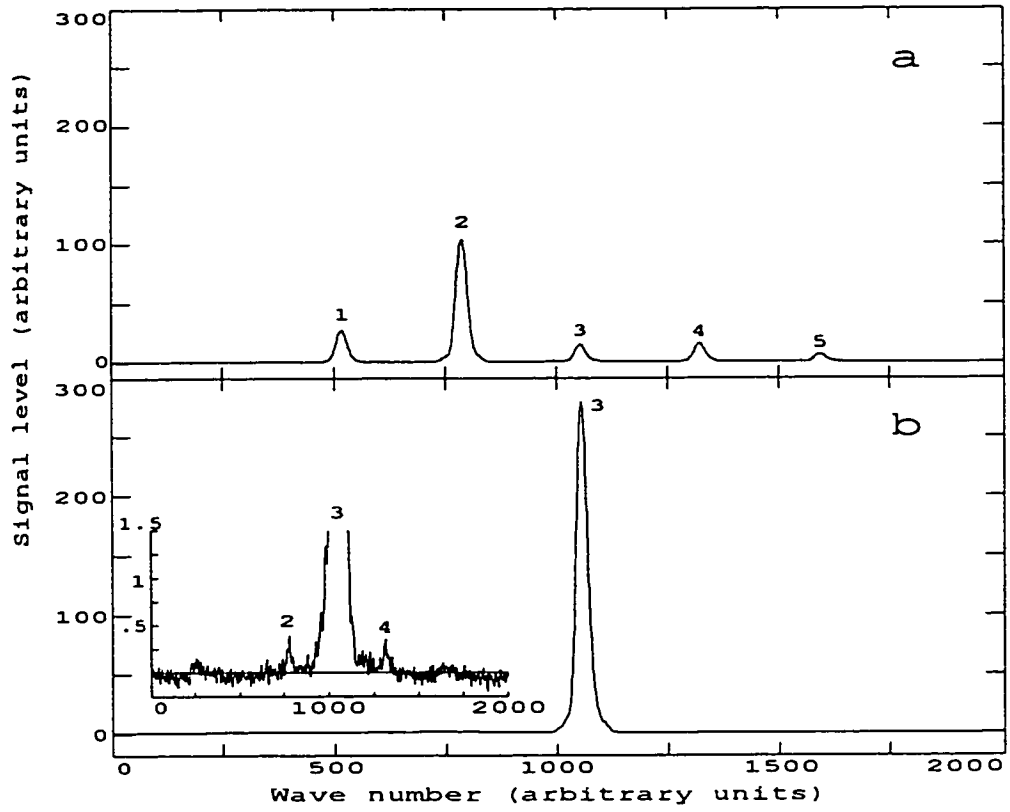

Figure 7: Mode profile of an InGaAsP laser: (a) without an external cavity mirror and (b) with feedback from a spherical mirror approximately 150 μm away from the laser. The inset (b) is expanded in the vertical position so that the side mode suppression ratio can be calculated. Modes are numbered from long to short wavelength. For all traces, the widths of the individual modes are instrument broadened.

The spectral output of an InGaAsP laser is shown in Fig. 7. Figure 7(a) shows the modes of a solitary laser, with the modes being numbered 1 to 5 from long to short wavelength. With the addition of a spherical mirror mounted on the flexure module, the laser operates essentially single mode as illustrated in Fig. 7(b). The insert window is expanded 200X in the vertical dimension and can be used to deduce the degree to which single mode operation is achieved. In this case, the ratio of the main lasing mode to the largest side mode is approximately 460. By adjusting the length of the external cavity, single-mode lasing could be obtained on any of the five numbered modes.

For applications which require single mode oscillation[34] and complete spectral coverage, one has to either use distributed feed back (DFB) or distributed Bragg reflector (DBR)-type lasers, which are very expensive, or devise a scheme to force normally multimode lasers to operate in a single mode.[24, 35, 36, 37, 38, 39, 40, 41]. The flexure module presented here is one scheme to obtain single mode semiconductor lasers. It is relatively easy to align the cavity mirror using this flexure system. The flexure system, however, needs occasional adjustment (once every five to seven weeks) when subjected to extensive fluctuation in the ambient temperature.

III-2 Frequency Tuning Technique

In this section, the experimental set-up to measure the change in the emission frequency of the laser as the position of the external cavity mirror is made to vary is described.

In a typical frequency tuning experiment, a normally multi-mode Fabry-Perot semiconductor laser is mounted onto a thermoelectric cooler. This cooler sets and maintains a constant operating temperature for the laser under study[31]. For all the measurements in this thesis the temperature was maintained at $25^0 C$.

Fig. 8 is a schematic diagram of the experimental set-up. In this set-up a short external cavity (SXC) laser module was formed by placing an external mirror ($\cong 200 \mu m$) behind the back facet of the laser. In a typical set-up the coupling factor x resulting from this arrangement is between 10^{-3} and 10^{-4}. The external mirror has dual purposes. First, the light reflected from this mirror back into the cavity of the laser forces the laser into single mode operation[24]. Second, by mounting this mirror on a piezoelectric transducer (PZT) the length of the short external cavity can be precisely controlled, and by slightly altering the length of the SXC, the experimenter can vary the resonant frequency of the laser. In this way, the experimenter can either scan across a single mode or move the mirror across a larger distance to select a different mode. To install this SXC mirror properly, the light output from the laser was first made to reflect off a mirror (M3) into a monochromator. The output from this monochromator allows the spectral output to be viewed in real time. The SXC mirror is positioned behind the laser in such a way that the spectrum of the laser exhibits single mode operation, with side mode suppression ratio (SMSR) $\geq$ 200. Once this is accomplished mirror M3 is removed.

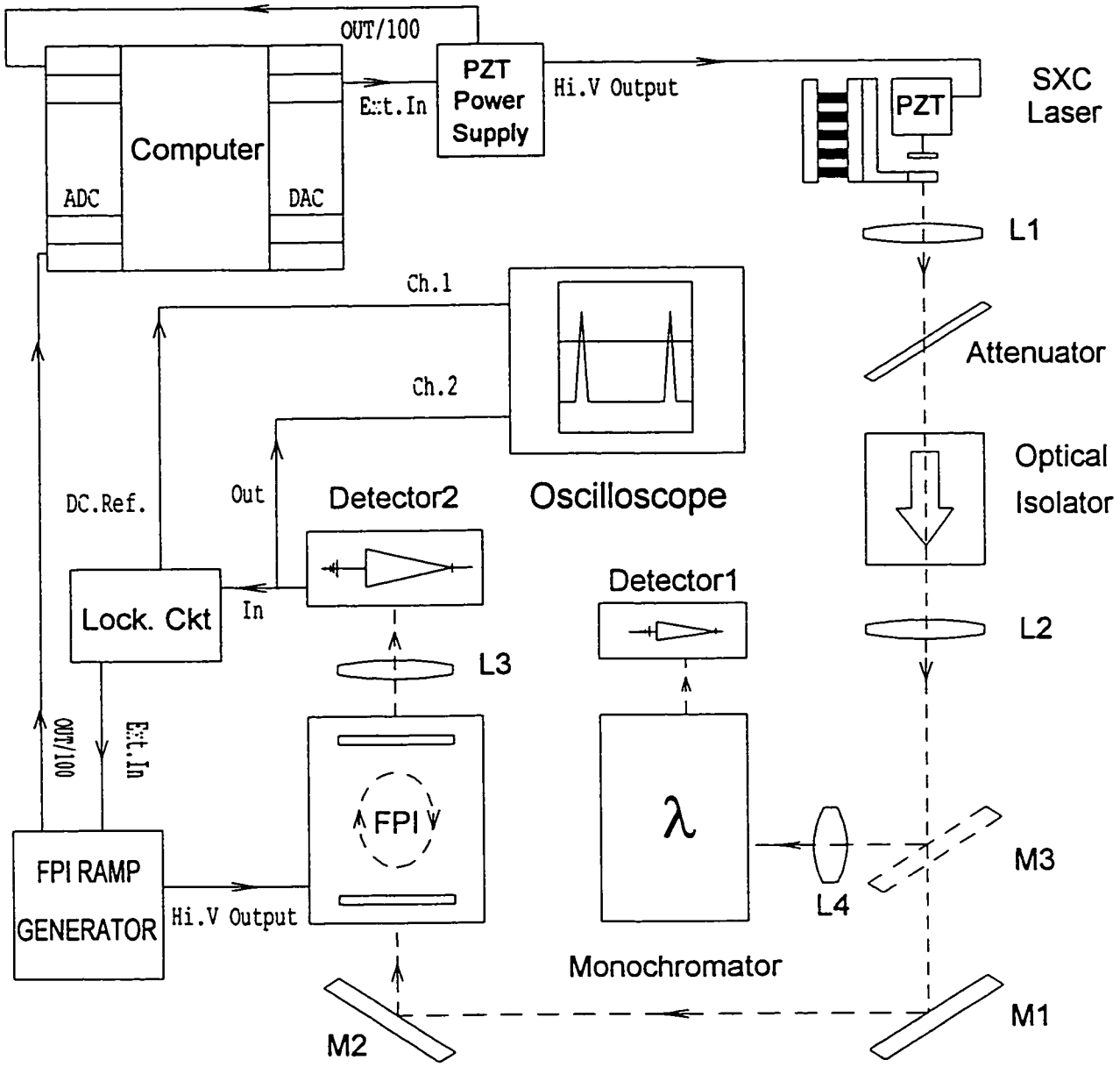

Figure 8: Optical apparatus and electronics configuration for the frequency tuning experiment.

The light output from this now single mode laser is collected by lens L1, passed through an optical attenuator and through an optical isolator. This combination of attenuator-isolator is there to reduce unintentional feedback through the front facet of the laser. The total optical isolation, provided by this combination, is approximately 60 dB to 70 dB. Following the optical path (the dashed line in Fig.8), the light that emerges from the optical isolator is eventually fed through a Fabry-Perot interferometer (FPI). The interferometer (Burleigh RC 140) employed dielectric-coated planar mirrors with 97% reflectivity. Fine control of the cavity length is provided by PZTs driven by a high voltage ramp generator (Burleigh RC-43). The output from this FPI is received by a photo-detector. From this detector, two electrical signals (the solid lines in Fig. 8) are sent out. The signal that is displayed on the oscilloscope allows the experimenter to align the FPI and to monitor the experiment once it is in progress. The other signal from the photo-detector goes to a custom-built lock circuit[31].

To start the experiment, a computer is used to send a ramp voltage to the high voltage supply. This supply, in turn, sends a voltage to the PZT crystal, which expands to push the SXC mirror forwards. The shortening of the length of the SXC induces a shift in the emission frequency of the laser. This frequency shift results in a change of the FPI fringes, which will be detected by the lock circuit. To respond to this change, the lock circuit sends an error voltage to the ramp generator of the FPI. This ramp generator, once it receives the signal from the lock circuit, will adjust the position of the FPI mirrors in such a way that this error voltage reduces to zero. In this way, the frequency shift of the laser is tracked. The same computer that is used to ramp the mirror of the SXC is also

used to receive the monitor signals from the PZT high voltage supply and from the FPI ramp generator. These monitor signals, after proper calibration, are converted to the change in the length of the short external cavity and the shift of the emission frequency, $(\nu - \nu_{nf})$, of the laser.

Once collected, a least-squares program is used to fit the data to Eq. (22). In this procedure, the original length l_x of the short external cavity, the linewidth enhancement factor α and the angular factor $\kappa(\theta,\varphi)$ of ξ (c.f. Eq. (5)) are all fitting parameters. It was found that as long as more than three longitudinal modes could be selected for measurements from the same laser, the α parameter of the laser could be determined in a consistent and reliable manner.

III-3 Summary

In this chapter, the construction of a short external cavity module based on the flexure mount concept is presented. The operation and the characteristics of the flexure mount are presented in some details. It was shown, with the use of an index-guided laser that by using the flexure mount a normally multi-mode semiconductor laser could be made to oscillate in a single mode, with a side mode suppression ratio $\geq$ 400. The SXC laser module was then used in the experimental set up, presented in the last section. The experimental set up allows the experimenter to vary the resonant frequency of the laser by simply changing the length of the short external cavity. Once the shift in the

frequency of emission is recorded, this data is used to derive the linewidth enhancement factor of the laser.

Measurements made with the equipment and technique described in this chapter are presented in the next chapter.

IV- Experimental Results and Discussion

In this chapter, to demonstrate the use of the technique developed in the last two chapters, measurements performed on an index-guided and a quantum well laser are presented. In the first section, typical frequency tuning curves obtained from these lasers are presented. Also in this section, the fitting procedure to extract the linewidth enhancement factors from these curves is explained in detail. In the second section of this chapter, the correlation between these linewidth enhancement factors and the linewidths of the lasers is reported. In the last section of this chapter, the effect of optical feedback on the linewidth enhancement factors of the lasers is discussed.

IV-1 Frequency Tuning Curves and Linewidth Enhancement Factors

A- An Index-Guided Laser

The index-guided InGaAsP laser (i.e. not a quantum well structure) used in this experiment is 250 μm long. This laser emits light at a wavelength of $\lambda = 1.3 \mu m$ and has a threshold current of 16.3 mA at room temperature ($25^0 C$). To form an SXC laser module, a spherical reflector was positioned $\cong$ 160 μm behind the back facet of the laser. This spherical mirror is made of polished aluminum, with its surface formed by impression of a precision ball bearing of 380 μm in diameter. When properly aligned, the optical feedback from this mirror forced the laser to oscillate on a single mode. A selection of seven different longitudinal modes was possible. The side mode suppression

ratio ranged from 240 to 320 at 20 mA injection current level, depending on the mode. The farther the mode is from the gain peak the poorer is the side mode suppression ratio.

Typical frequency tuning curves obtained for this laser at 20 mA are shown in Figs. 9, 10 and 11. In these figures, the SXC mirror is moved in the direction of decreasing external cavity length l_x, and the frequency axis displays the shift of the emission frequency of the laser from its original value (i.e., before the resonant frequency is varied). It should also be noted that, in this thesis, the modes of the laser are numbered in order of decreasing wavelength. Presented here, mode 4 is nearest to the gain peak of the laser, while modes 3 and 5 bracket the gain peak with mode 3 on the longer wavelength side.

From these three figures it can be seen that as the phase of the optical feedback changed (by shortening the length l_x of the SXC) the emission frequency of the laser went through an initial red shift, followed by a blue shift. However, the difference is that the mode on the blue side of the gain peak of the laser (mode 5) experiences a net blue shift while the mode on the red side (mode 3) experiences a net red shift, before mode hopping occurred at the end of the experiment. The smooth curves drawn through the experimental data in these graphs are generated by the fitting procedure.

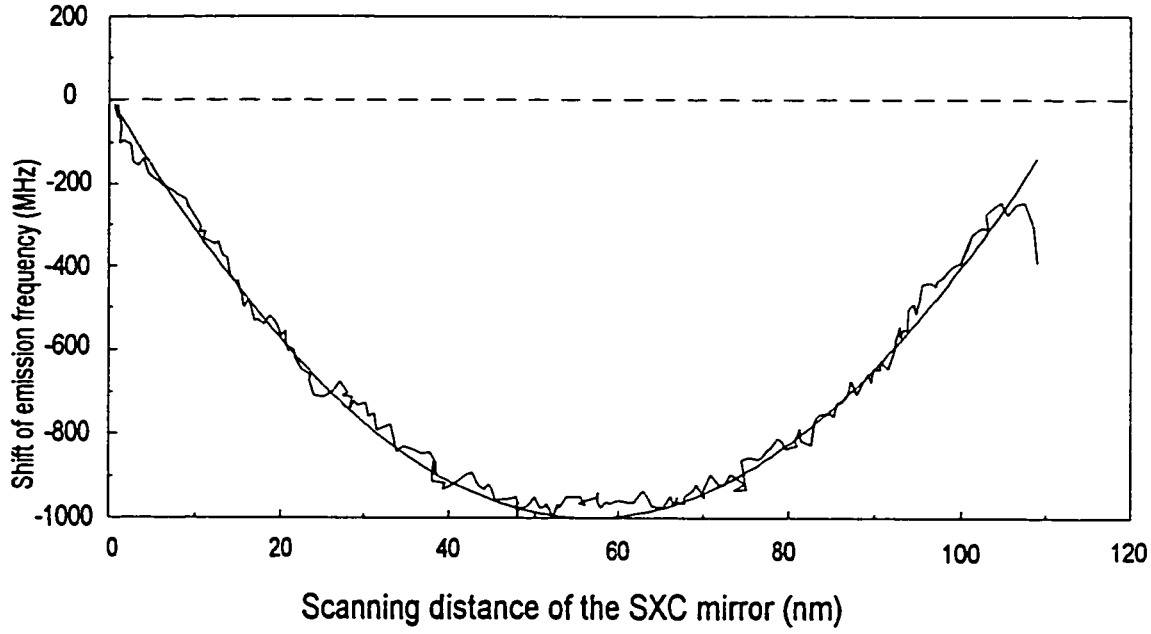

Figure 9: Frequency tuning of mode 3 (on the long wavelength side of the gain peak).

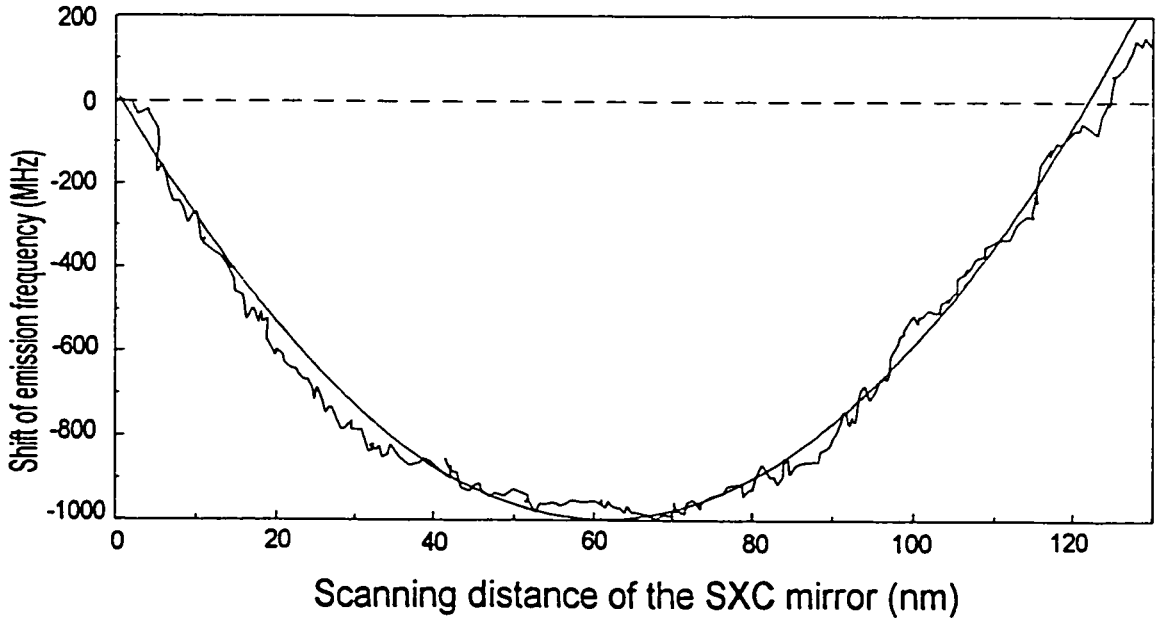

Figure 10: Frequency tuning of mode 4 (on the gain peak).

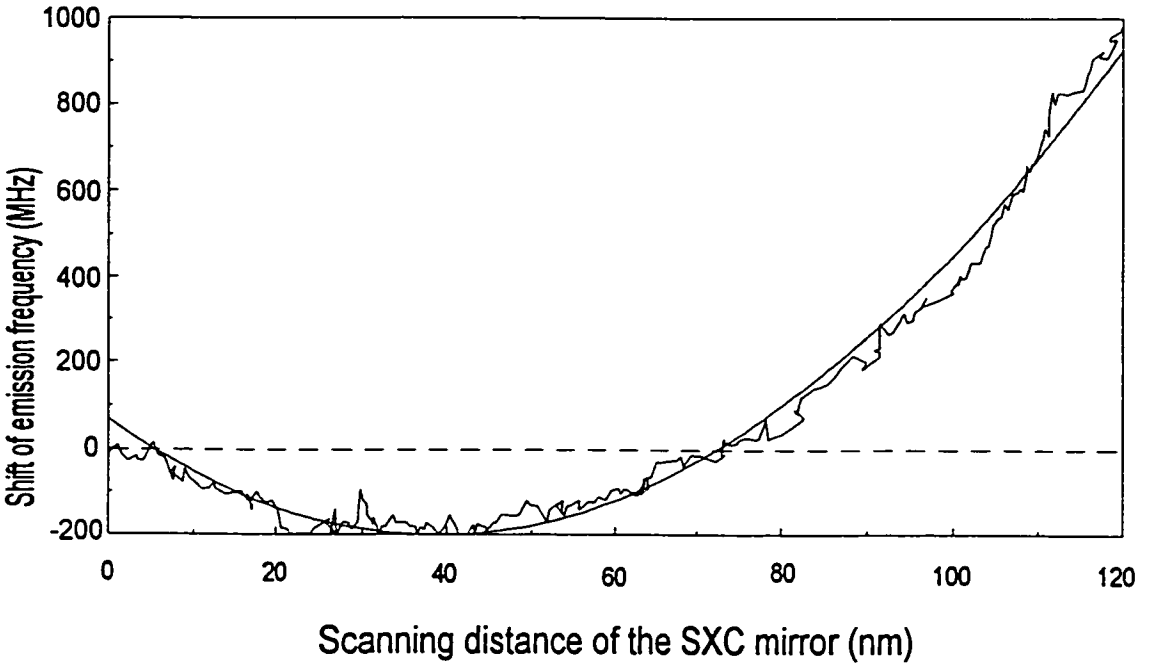

Figure 11: Frequency tuning of mode 5 (on the short wavelength side of the gain peak).

To fit the collected data to Eq. (21) a procedure was carried out as follows: a mode is chosen at random and the frequency tuning data is used in what is termed "the primary fit". In this fit, the independent variable δl_x is fitted against the dependent variable $(\nu - \nu_{nf})$. The angular factor $\kappa(\theta,\varphi)$, the linewidth enhancement factor α, the wavelength of emission λ, and the initial SXC length l_x of the laser were all allowed to vary independently. The fitting procedure varies these parameters, within boundaries imposed by the physics of the system, to minimize χ^2 for the best fit[42]. At the end, the results of this primary fit were kept to be used as a basis in all the subsequent fits. In the fitting of all the remaining longitudinal modes of the same laser, the angular factor

$\kappa(\theta,\varphi)$, obtained in the primary fit, was kept constant. Knowing the length of the laser, the emission wavelength of the mode being fitted can be calculated from the wavelength of the mode used in the primary fit. Similarly, the length, l_x, of the SXC at the start of any scan, can also be determined by the fitting results of the primary mode. This way, in the fitting of all the remaining modes the only parameter allowed to vary is the linewidth enhancement factor α.

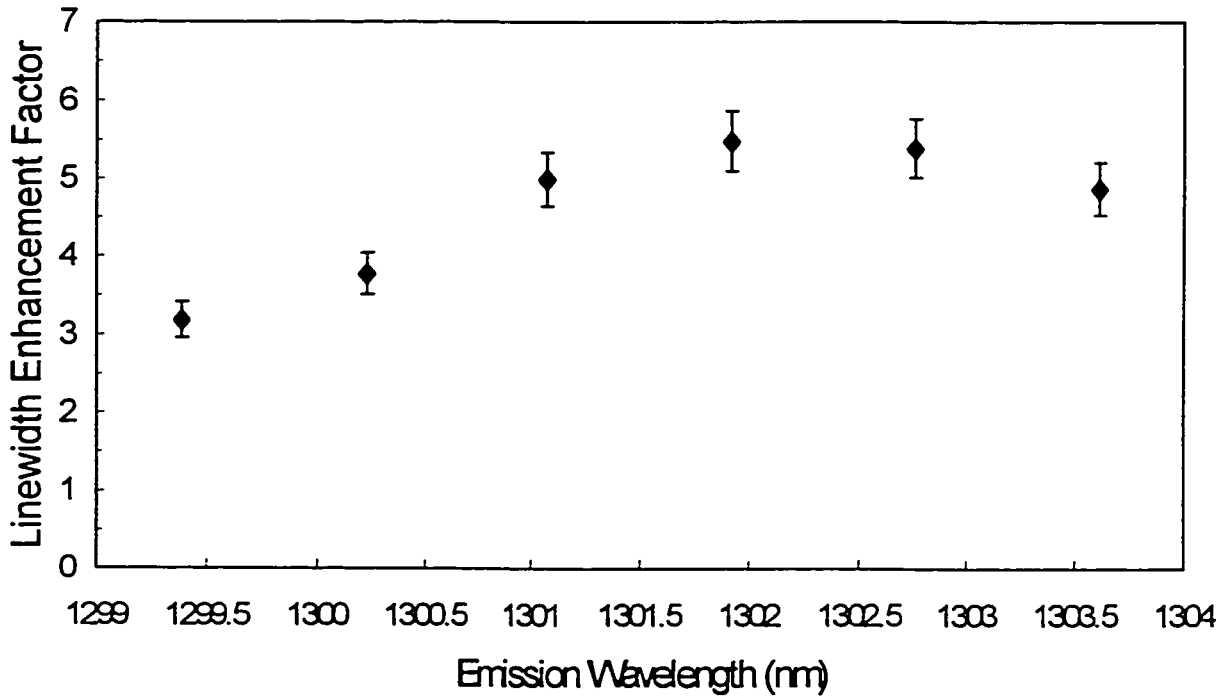

Figure 12: Linewidth enhancement factors versus emission wavelength for an index-guided laser.

The graph of linewidth enhancement factors versus wavelength is presented in Fig. 12. The six data points shown in this graph represent the first six longitudinal modes

that could be selected using the external cavity mirror (Mode 7 was too far from the gain peak, therefore, the frequency tuning curve has a low SNR.). The linewidth enhancement factors found for each of these modes are plotted against the wavelength of emission.

From this graph, it can be seen that the linewidth enhancement factors ranged from 3.2 to 5.5, depending on the mode. This wavelength dependence of alpha factors has been observed before[43, 44, 45]. For this laser, mode 4 has a maximum linewidth enhancement factor.

B- A Multi Quantum Well Laser

The second laser that was used to test the experimental method is a quantum well laser. This laser was designed and fabricated by a research group at McMaster University[46]. The active region of this laser consists of ten 35 Å quantum wells. These wells are separated by nine 100 Å barrier layers and the band gap of the barriers was reported to be 1.10 μm. The laser emits at a wavelength of 1.291 μm. At room temperature this laser has a threshold current of 23.5 mA. As in the previous case, the same aluminum spherical mirror was used to provide optical feedback. Once properly aligned, the feedback from this mirror allowed a selection of six individual longitudinal laser modes. At an injection current of 29.0 mA, the side mode suppression was found to be between 180 and 280, depending on the mode. Frequency tuning experiments were performed on all these modes at the above injection current. The frequency tuning curves obtained for this laser have similar characteristics to those of the index-guided laser, presented in the last section. Therefore, they are not presented here.

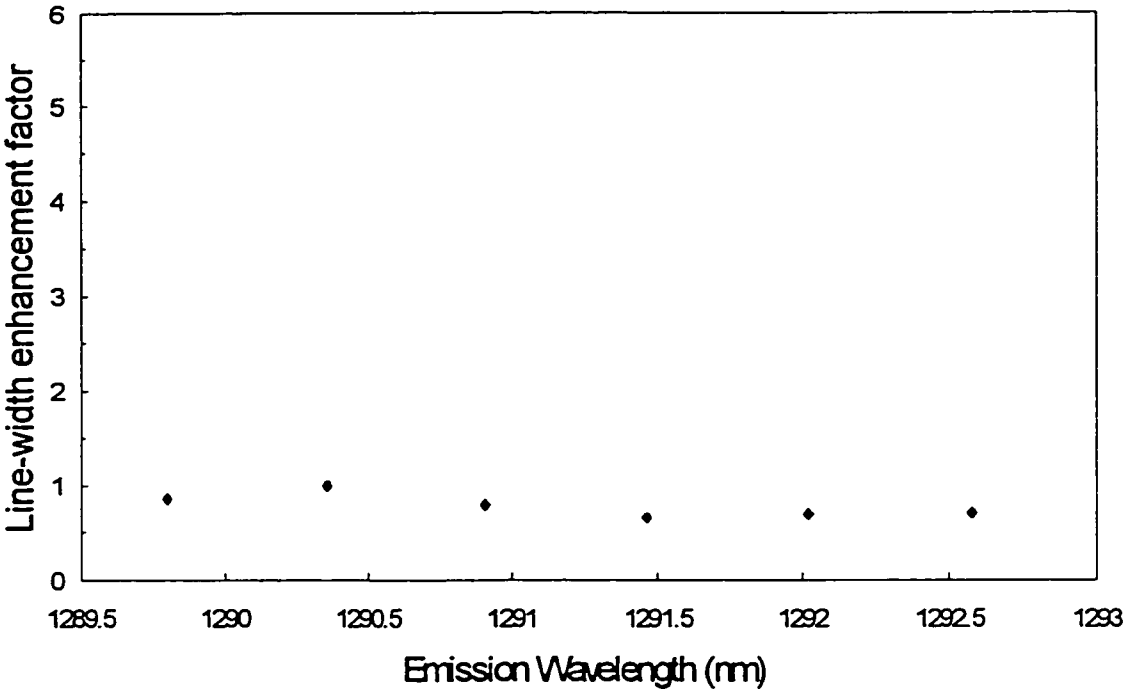

Figure 13: Linewidth enhancement factors versus emission wavelength of a multi-quantum well laser. The values of the uncertainties are between 4% to 6% (too small to show on the graph).

The collected data for this laser is analyzed by the same method explained earlier. In Fig. 13 the linewidth enhancement factor obtained for each longitudinal mode is plotted against the wavelength of emission.

It should be noted that, in Fig. 13, the graph is presented with the same scale used in Fig. 12. This is for the ease of comparison between the two figures. At a glance, the modal dependence of the α parameter for this laser is the same as that of the index-guided laser. Around the gain peak of the laser (found at mode 2, the second shortest

wavelength mode), the linewidth enhancement factor attains its maximum value, and this value gently rolls off as the mode moves farther away, in either direction. The important difference is, however, that the average value of the linewidth enhancement factors of this laser is smaller than that of the index-guided laser. This smaller α is to be expected for a multi-quantum well laser[47]. Also from Fig. 13, it seems that the linewidth enhancement factor starts to flatten out and even increases slightly at modes 5 and 6.

For each laser reported in this thesis, frequency-tuning data were collected in four sets of measurements. These sets of measurements were performed independently and each time with the SXC mirror re-aligned. Within a set, a single value of the linewidth enhancement factor is obtained from the fitting of a frequency-tuning curve. Each frequency-tuning curve consists of 300 data points, with each point averaged over 24 times by the computer. The error bars shown in the figures represent the spread of the fitted α parameter over the four sets of measurements.

IV-2 Linewidths and Linewidth Enhancement factors in Semiconductor Lasers

It was found in other works that the linewidth enhancement factor and the linewidth have the following relationship[10]: $\Delta\nu \approx (1+\alpha^2)$. Therefore, as a confirmation of this technique I carried out independent linewidth measurements[13, 31, 48] for these lasers and compared these data with the linewidth enhancement factors presented earlier.

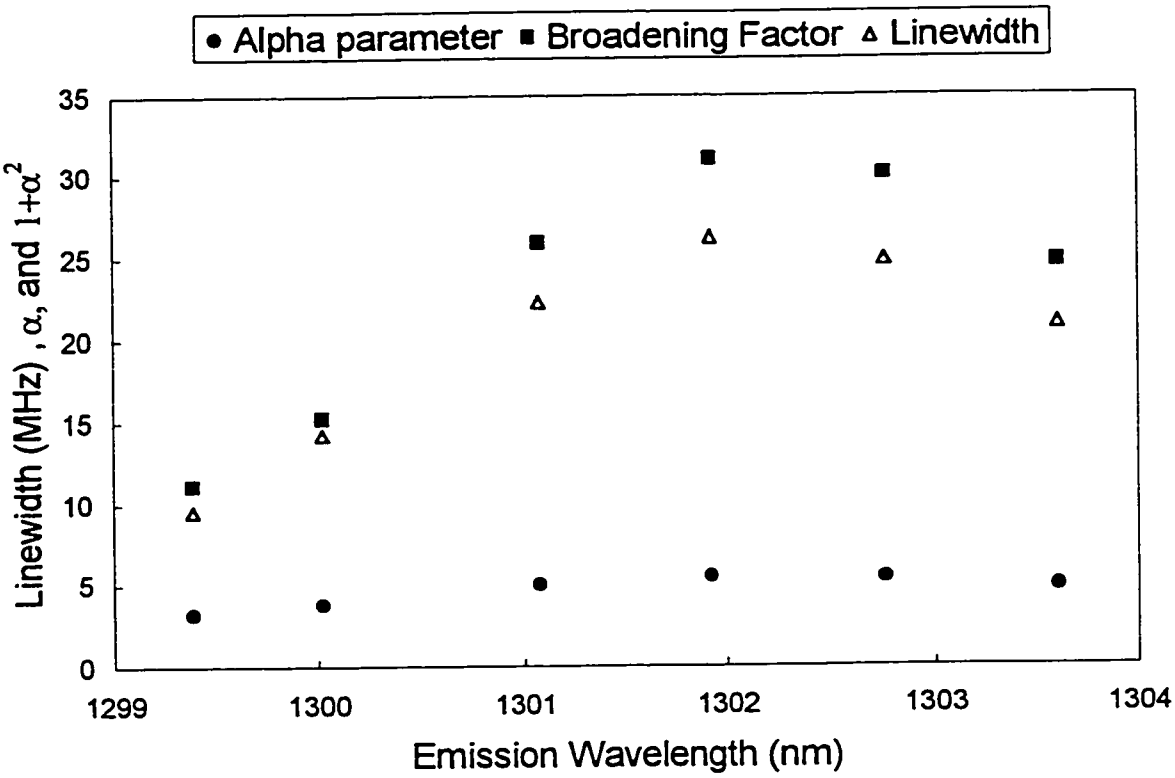

Figure 14: Correlation between linewidth enhancement factors and linewidth of the index-guided laser.

In Fig. 14, the values of linewidth enhancement factors (or the α-parameter), the broadening factor $(1+\alpha^2)$ and the linewidths $\Delta\nu$ of the index-guided laser were plotted against the emission wavelength λ. It is clear from this graph that the linewidth $\Delta\nu$ and the broadening factor $(1+\alpha^2)$ follow each other closely. The correlation coefficient between these two series was found to be 0.88.

Similar results were plotted for the quantum well laser in fig. 15.

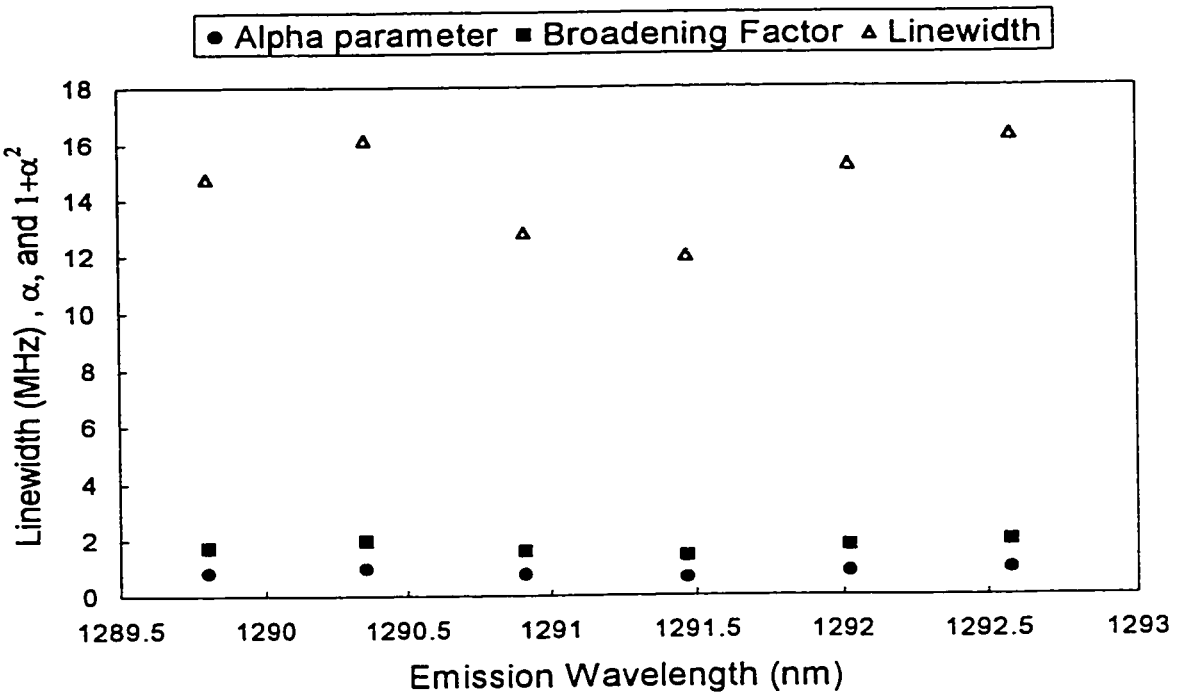

Figure 15: Correlation between linewidth enhancement factors and linewidth of the quantum well laser.

In figure 15, the values of linewidth enhancement factors (or the α-parameter), the broadening factor $(1+\alpha^2)$ and the linewidths $\Delta\nu$ were plotted against the emission wavelength λ of the quantum well laser. In this case, the correlation coefficient between $(1+\alpha^2)$ and $\Delta\nu$ was found to be 0.92.

These coefficients indicate that, in both cases, there is $\rangle$ 95 % chance that the two quantities in question are linearly correlated[42]. The linear correlation between the

broadening factors $(1+\alpha^2)$ and the linewidths $\Delta\nu$ of the lasers, which were measured independently, confirms the validity of this experimental method.

IV-3 Linewidth Enhancement Factors and Optical Feedback in SXC Laser

Although external cavities have been used on semiconductor lasers before, most previous works have been with long cavity configurations designed for linewidth reduction[49, 50, 51, 52, 53, 54]. In this section, experimental data will be presented to show that the short external cavity used in this thesis was introduced without significantly affecting the intrinsic properties of the laser. This allows the natural linewidth enhancement factor of the solitary laser to be measured faithfully.

To study the effect of the short external cavity mirror on the linewidth enhancement factors of the laser, measurements of the tuning of the emission frequency were carried out, with the mirror positioned at various distances from the back facet of the laser. The linewidth enhancement factors derived from these different configurations were then compared.

For the index-guided laser, the external cavity mirror was first positioned at about $160\mu m$ from the back facet of the laser. This configuration resulted in six longitudinal modes. The side mode suppression ratio ranged from 240 to 320 at 20 mA injection current level, depending on the mode (see section A of IV-1). Frequency tuning measurements were performed on these modes, and the linewidth enhancement factors were derived from this data. Next, the short external cavity mirror was moved to about

$210\mu m$ and $260\mu m$ from the back facet of the laser. In these two configurations, 5 and 4 longitudinal modes were obtained, respectively. Measurements were repeated for these two configurations. Care was taken to ensure that in all three configurations the side-mode suppression ratios were similar. This procedure was repeated many times and the data obtained could be divided into two cases. In the case where the SXC mirror was not very well aligned (when the side-mode suppression ratios of some modes are less than 250) a change in the SXC length resulted in a significant change of the α parameters. In the case where the SXC mirror is well aligned the linewidth enhancement factors remained constant (within experimental uncertainty) in all three configurations.

A set of linewidth enhancement factors obtained from three SXC mirror configurations are presented in Fig. 16.

The data in Fig. 16 represent one of the best cases. In this case, the side-mode suppression ratios of all the modes obtained from three different SXC mirror configurations were at least 320.

In this figure, "Short Config." corresponds to the case where the external mirror was at $160\mu m$ from the back facet of the laser. "Medium Config." and "Long Config." resulted from the configurations where the mirror was positioned at $210\mu m$ and $260\mu m$ from the back facet of the laser, respectively. The error-bars, which correspond to the uncertainties of 6%, are shown for the $160\mu m$ -configuration.

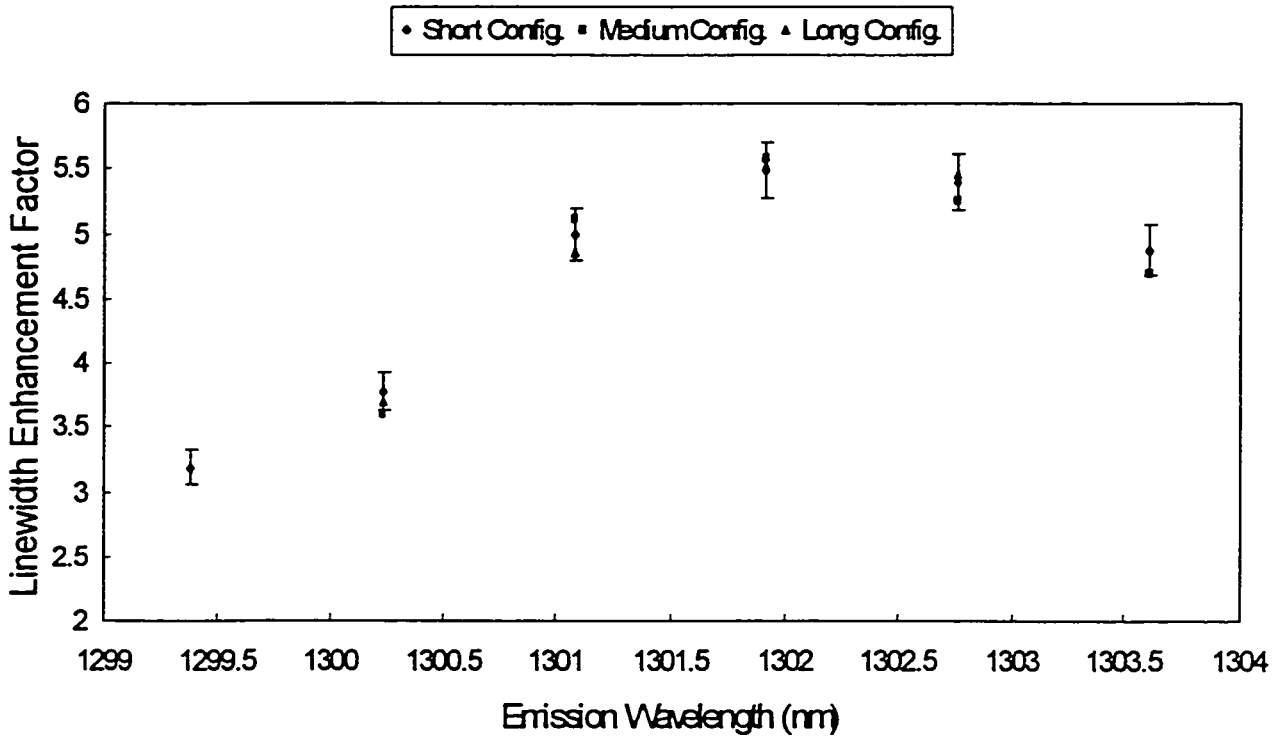

Figure 16: Linewidth enhancement factors of the index-guided laser with different short external cavity configurations.

The same procedure was then carried out for the quantum well laser, and the results are presented in Fig.17.

In this figure, "Short Config." corresponds to the case where the external mirror was at $260\mu m$ from the back facet of the laser. "Medium Config." and "Long Config." resulted from the configurations where the mirror was positioned at $310\mu m$ and $360\mu m$ from the back facet of the laser, respectively. The error-bars, which correspond to the uncertainties of 6%, are shown for the $260\mu m$ -configuration. The side mode suppression ratios ranged from 280 to 370.

From Fig. 16 and Fig. 17, it can be seen that if the SXC mirror is well aligned, then the linewidth enhancement factors derived from different short external cavity configurations for both the index-guided and the quantum well laser were within the uncertainties inherent in the experimental method.

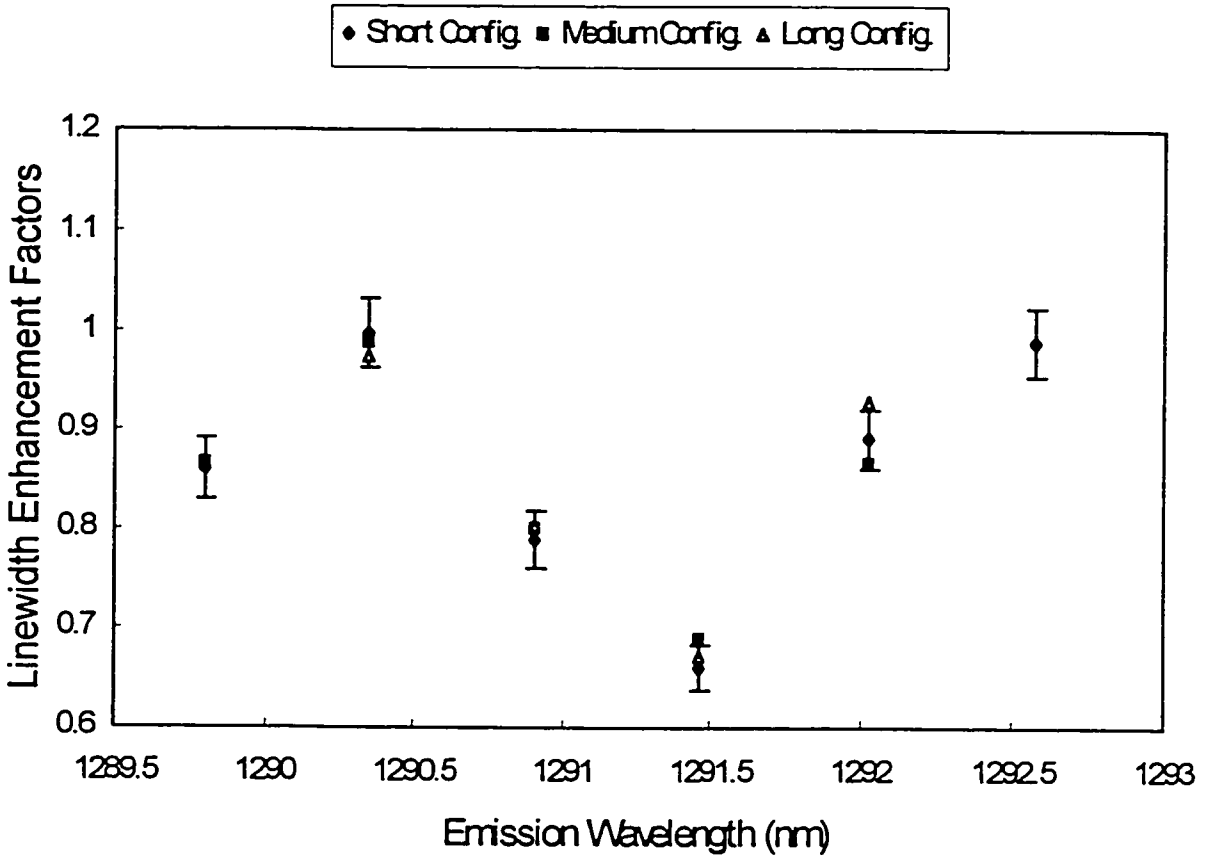

Figure 17: Linewidth enhancement factors of the quantum well laser with different short external cavity configurations.

The results presented in the last two figures indicate that although the scanning of the SXC mirror over a small distance (in the range of nanometers) alters the resonant condition of the laser, the magnitude of the linewidth enhancement factor is not directly affected by the level of optical feedback from this mirror.

IV-4 Summary

The theoretical framework and the experimental method, developed in the last two chapters, have been used to study the linewidth enhancement factors of two diode lasers in this chapter.

The linewidth enhancement factors of both lasers are wavelength-dependent. For the index-guided laser, it was found that the linewidth enhancement factors ranged from 3.2 to 5.5, depending on the mode. For the quantum well laser, the linewidth enhancement factors are much smaller, ranging from 0.7 to 1.1. This smaller α is to be expected for a multi-quantum well laser[47].

Independent linewidth measurements were also performed on these lasers. In both cases, the values of these linewidths follow the broadening factors $(1+\alpha^2)$ very closely. For both lasers, the linear correlation coefficients indicated that there is a more than 95 % chance that the linewidths and the corresponding broadening factors are linearly correlated.

Finally, by positioning the SXC mirror at various distances from the back facets of the lasers, it was confirmed that the optical feedback from this mirror does not alter the

magnitude of the linewidth enhancement factors. Thus, the values obtained were the natural linewidth enhancement factors of the lasers under test.

Having verified the validity of the experimental technique, it was then used to study the linewidth enhancement factors for a series of multi-quantum well lasers. These lasers have different barrier compositions. The experimental findings are reported in the next chapter of this thesis.

V- Linewidth Enhancement Factors in Multi-Quantum Well Lasers with Varying Barrier Height

V-1 Some Background on Quantum Well Devices

A quantum well structure consists of one or more very thin layers of a relatively narrow bandgap semiconductor interleaved with layers of a wider bandgap semiconductor. The thickness of these layers is typically 100 Å or less[55]. An arrangement like that shown in Fig. 18, with many layers, is called a multiple quantum well (MQW) structure. These required layers could be grown by either Molecular Beam Epitaxy (MBE), or Metal-organic Chemical Vapor Deposition (MOCVD) techniques.

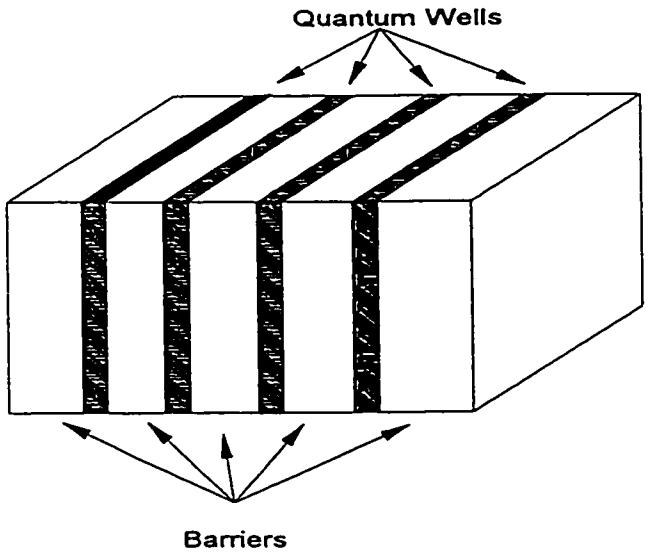

Figure 18: Multiple quantum well structure.

The special properties of these very thin layers result from the confinement of carriers (electrons and holes) in a manner analogous to the well-known quantum problem of the "particle in a box"[56]. In this case, the carrier is confined to the narrow bandgap wells by the larger bandgap barriers. Since the quantum wavefunctions of the carriers must approach zero at the barriers and form a standing wave pattern within the wells, only a certain number of discrete "energy states" are allowed for the carriers (see Fig. 19). The motion of the carriers is quantized.

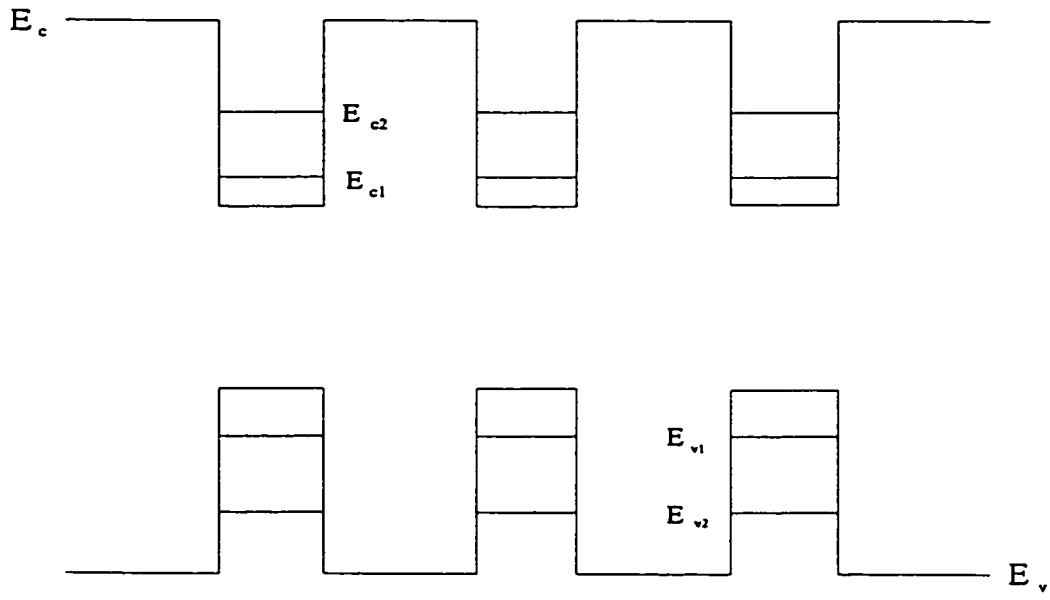

Figure 19: Energy Diagram of a MQW structure

In laser diodes, a high gain requires population inversion of levels with a high density of states. In a bulk laser, this can only be achieved after first filling the lower lying energy levels. In quantum well lasers, where the electron and hole energies are

quantized into discrete levels within the energy wells, the peak gain is associated with levels at the bottom of the bands[57]. This fact reduces the number of carriers needed to achieve a given level of population inversion. As a consequence, the threshold current of the quantum well laser is reduced, as compared to that of a conventional laser diode. Another main difference between bulk and quantum well lasers is that the density of states increases as $A(\hbar\omega - E_g)^{1/2}$ in bulk lasers, while in quantum well lasers it rises abruptly from zero to $A(E_1)^{1/2}$ for $\hbar\omega \geq E_1 + E_g$. The sudden and large onset of the gain at this point causes a discontinuous drop in the refractive index, and both factors contribute to reducing the linewidth enhancement factor α in quantum well lasers[34]. There have been many theoretical calculations, and much experimental evidence showing that the α parameter is substantially smaller in quantum well lasers as compared to that of the bulk lasers[58, 59, 60].

Quantum well lasers are both physically interesting and technologically important. Quantum well technology allows the crystal grower to engineer the number, the range, the depth, and the arrangement of quantum mechanical potential wells. The control over these parameters can be used not only to study the physics of the devices but also to manufacture very good lasers. Therefore, during the last few years there have been many investigations, aiming to determine which parameters most affect the linewidth enhancement factor[44, 61, 62] and thus the performance of the laser.

In the next sections of this chapter, experimental data collected from a series of five MQW lasers are presented. These data reveal the dependence of the linewidth

enhancement factors on the wavelength of emission on the depth of the well barrier, and on the output power of these lasers.

A research group at McMaster University[46, 63] designed and fabricated the lasers used in this chapter. These lasers were made for operation at about $1.3\mu m$, and were grown epitaxially by the MOCVD technique on InP wafers. The active region of these lasers consists of ten 35 Å quantum wells, and the composition of the QW material was nominally the same in all five lasers. The quantum wells are separated by nine 100 Å barrier layers. The composition of these layers was varied to realize five barrier depths, ranging from 1.03 to 1.24 eV.

V-2 Dependence of the Linewidth Enhancement Factor on the Wavelength of Emission in InGaAsP Multi-quantum Well Semiconductor Lasers

In this section, the linewidth enhancement factors obtained from five MQW lasers are plotted against their wavelength of emission. The lasers are referred to by the name of the structure used by the manufacturers[46, 63]. As in chapter IV, the modes of the lasers are numbered in the order of decreasing wavelength,

A- S1-592

The first laser reported in this section is from wafer S1-592. This laser is $375\mu m$ long, and has a threshold current of 24 mA when operated at $25^{0}C$. The laser emits at a wavelength of $1.327\,\mu m$ and the band gap of the well barriers was reported to

be 1.03 eV[46]. To form an SXC laser module, a spherical reflector was positioned behind the back facet of the laser. A selection of six different longitudinal modes was possible. The linewidth enhancement factors obtained from these modes are presented in Fig. 20.

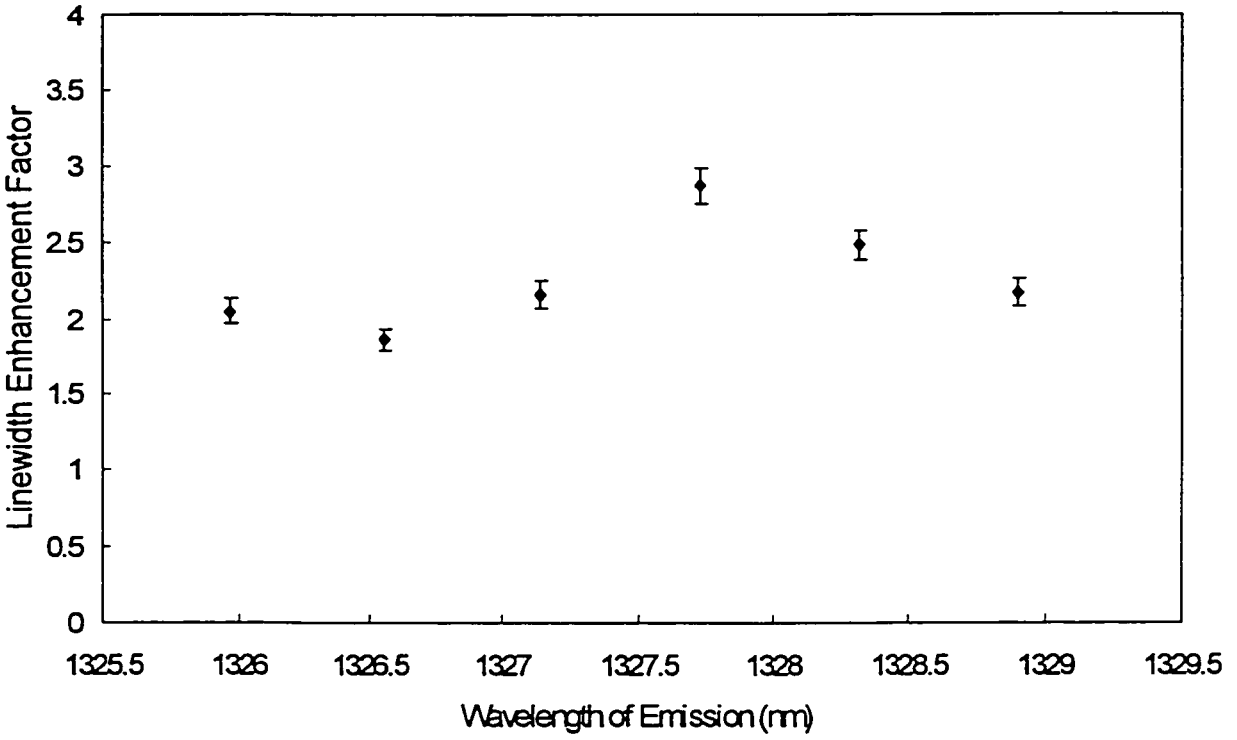

Figure 20: Linewidth Enhancement Factors of S1-592. Mode 3 is near the gain peak of the laser.

B- S1-590

The second laser is from wafer S1-590. This laser is 375μm long, and has a threshold current of 28 mA when operated at 25$^{\circ}C$. This laser also emits at a wavelength of 1.327μm and the band gap of the well barriers was reported to be 1.08

eV[46]. To form an SXC laser module, the same spherical reflector was positioned behind the back facet of the laser. A selection of six different longitudinal modes was possible. The linewidth enhancement factors obtained from these modes are presented in Fig. 21.

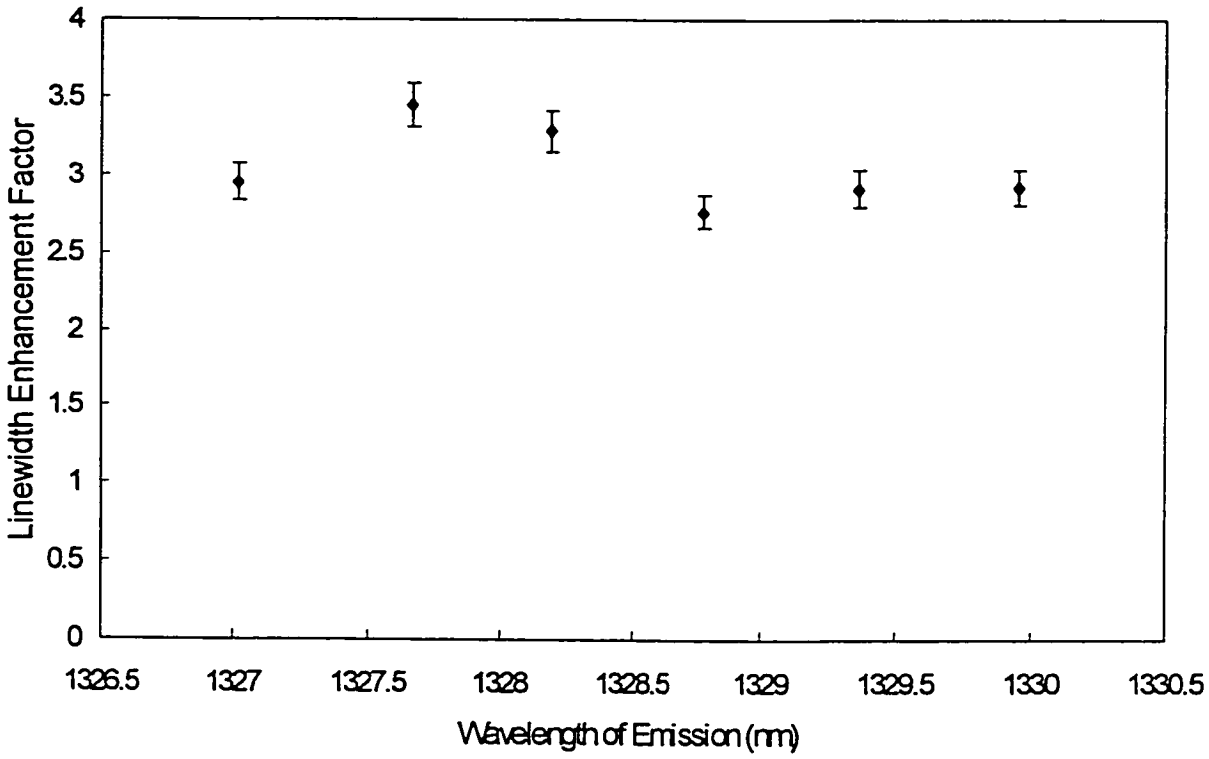

Figure 21: Linewidth Enhancement Factors of S1-590. Mode 5 is near the gain peak of the laser.

C- S1-588

The third laser is from wafer S1-588. This laser is $375\mu m$ long, and has a threshold current of 23.5 mA when operated at $25^{\circ}C$. This laser emits at a wavelength

of 1.291 μm and the band gap of the well barriers was reported to be 1.13 eV[46]. To form an SXC laser module, the spherical reflector was positioned behind the back facet of the laser. A selection of six different longitudinal modes was possible. The linewidth enhancement factors obtained from these modes are presented in Fig. 22.

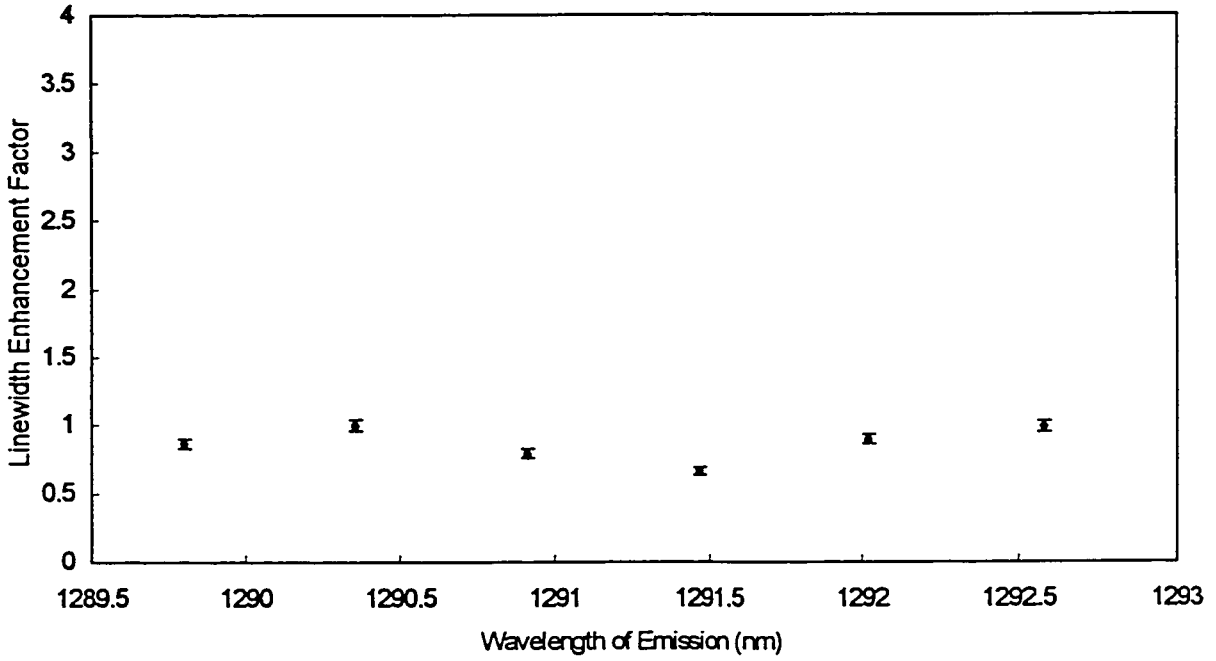

Figure 22: Linewidth Enhancement Factors of S1-588. Mode 5 is near the gain peak of the laser.

The data for this laser was reported in section IV-1 of this thesis. It is presented here again for the convenience of the reader and for the ease of comparison with other lasers in the group.

D- S1-593

The fourth laser is from wafer S1-593. This laser is $375\mu m$ long, and has a threshold current of 33.4 mA when operated at 25^0C. This laser emits at a wavelength of $1.284\,\mu m$ and the band gap of the well barriers was reported to be 1.18 eV[46]. To form an SXC laser module, the spherical reflector was positioned behind the back facet of the laser. A selection of six different longitudinal modes was possible. Their linewidth enhancement factors are presented in Fig. 23.

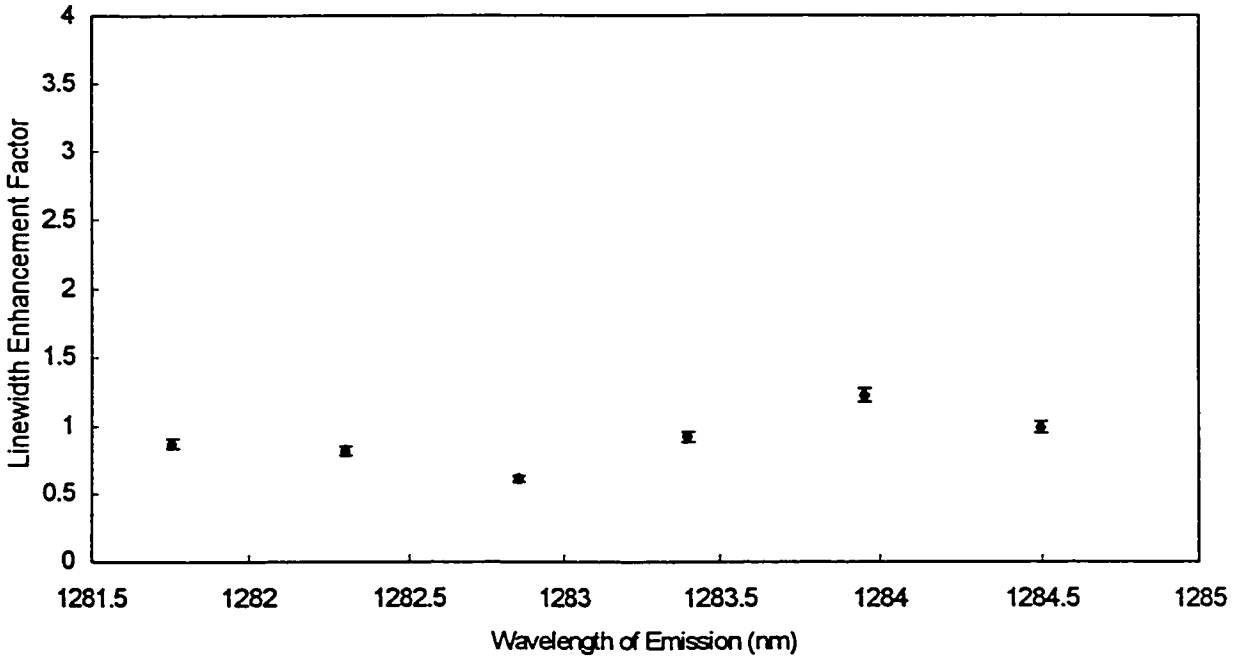

Figure 23: Linewidth Enhancement Factors of S1-593. Mode 2 is near the gain peak of the laser.

E- S1-591

The last laser is from wafer S1-591. This laser is 375μm long, and has a threshold current of 48.6 mA when operated at 25^{o}C. This laser emits at a wavelength of 1.27μm and the band gap of the well barriers was reported to be 1.24 eV[46]. To form an SXC laser module, the spherical reflector was positioned behind the back facet of the laser. A selection of six different longitudinal modes was possible.

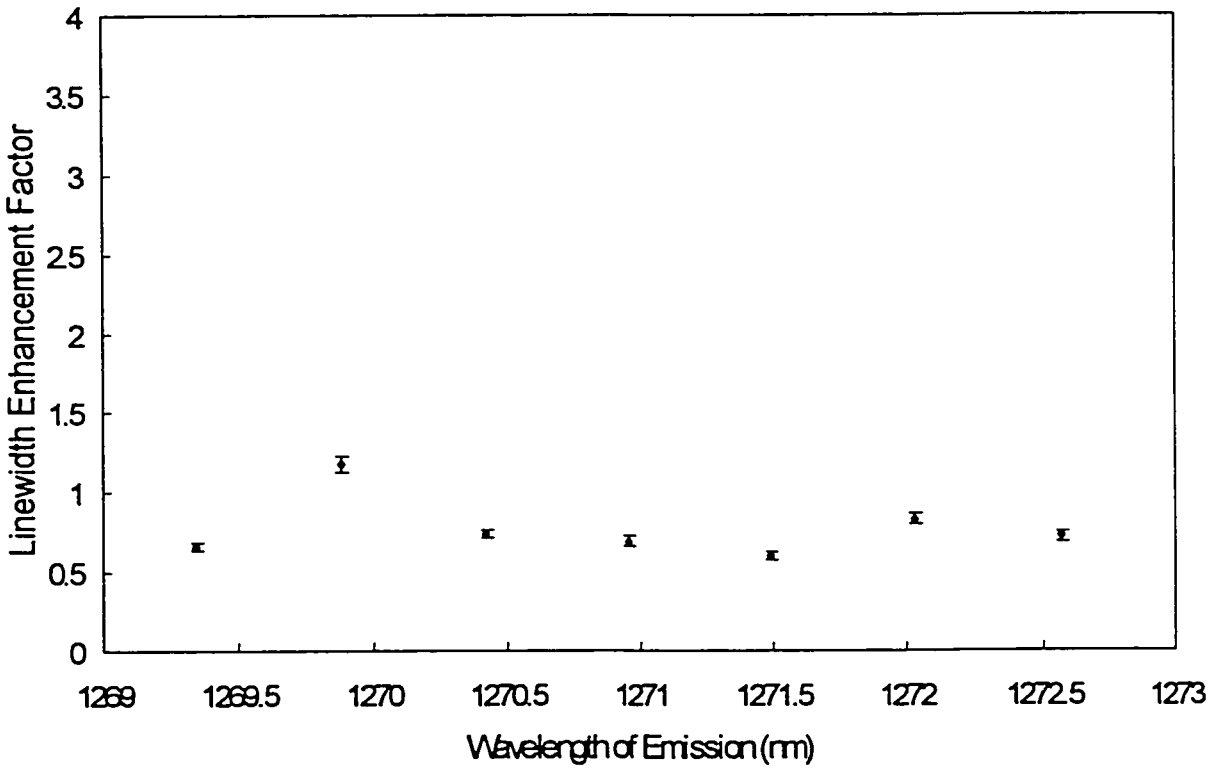

Figure 24: Linewidth Enhancement Factors of S1-591. Mode 2 is near the gain peak of the laser.

From the data presented in this section, the dependence of the linewidth enhancement factors on the wavelength of emission for all five lasers has been observed. Similar to the case of the index-guided laser presented in chapter IV of this thesis, the linewidth enhancement factors attain their maximum values around the gain peaks of the MQW lasers, and these values gently roll off as the modes move farther away, in either direction. There are, however, two important differences. The first difference is that the α factors of the MQW lasers seem to be less dependent on the wavelengths of emission than that of the index-guided laser. As one scans over the modes of the index-guided laser the difference between the largest and the smallest α factor is nearly 3 while in the MQW lasers, this difference is much smaller. The second difference is that in the quantum well lasers, as the mode moves far away from the gain peak the linewidth enhancement factors after the initial decrease start to increase again. This increase was not observed in the index-guided laser.

V-3 Dependence of the Linewidth Enhancement Factor on the Band Gap of the Well-barrier in InGaAsP Multi-quantum Well Semiconductor Lasers

To study the relationship between the linewidth enhancement factors and the band gaps of the well barriers, frequency-tuning experiments were performed on these lasers at the same output power, 2.5 mW. The linewidth enhancement factors thus obtained are plotted against the band gaps of the well barriers in Fig. 25.

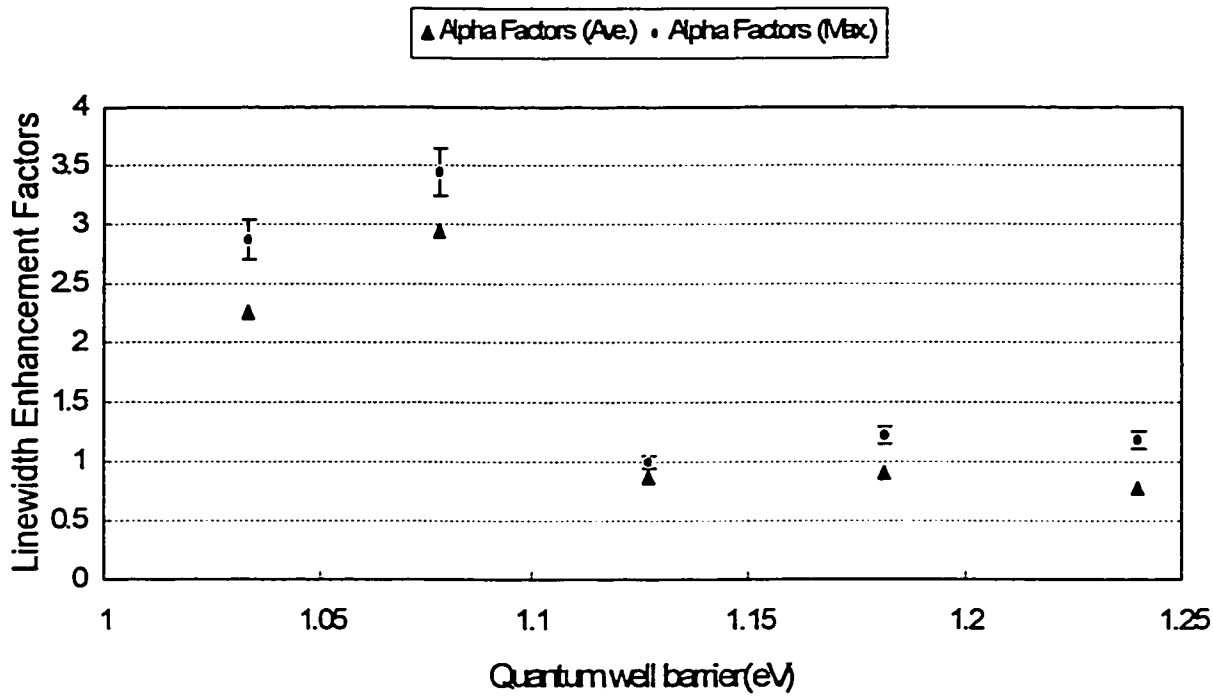

Figure. 25: Linewidth enhancement factors versus band gap of the well barrier.

In Fig. 25, the α parameters obtained from the modes that oscillate on the gain peak of each laser are presented as "Alpha Factors (max)". The error bars corresponding to 6% relative error are shown for this series. In the other series, a single data point represents the α parameters averaged over all modes for each laser.

Yariv and coworkers studied the effect of varying the barrier height on GaAs lasers[6]. In their study they concluded that as the height of the well barrier increases the linewidth enhancement factor of the laser also increases. They attributed this trend to the state filling effect.

From Fig. 25 of this thesis, one can see that the results obtained for the InGaAsP quantum well lasers follow a similar trend. Starting from the left of the figure, it is seen

that as the height of the well barrier increases from 1.03 eV to 1.08 eV the linewidth enhancement factor also increases. After this point, there is a sudden drop in the linewidth enhancement factor, and then the linewidth enhancement factor again follows the increase of the well barrier from 1.13 eV to 1.24 eV, for the last three lasers.

The abrupt change in the linewidth enhancement factor, seen in Fig. 25, can be explained as followed: It is known that the carriers are not evenly distributed across the active region of a MQW laser[64] and this effect becomes more pronounced as the height of the well barrier increases. I suspect that as the height of the well barrier increases from 1.08 eV to 1.13 eV the effect of this non-uniform carrier distribution becomes strong enough to alter the operating characteristics of these lasers.

Wafer.	Band gap of the barrier (eV).	Threshold current (mA).	Emission Wavelength (μm).	Linewidth Enhancement Factor (α).
S1-592	1.03	24.0	1.327	2.87
S1-590	1.08	28.0	1.327	3.45
S1-588	1.13	23.5	1.291	0.99
S1-593	1.18	33.4	1.284	1.23
S1-591	1.24	48.6	1.270	1.18

Table 1: Linewidth Enhancement Factors of MQW lasers with varying barrier height.

To examine the abrupt change of the linewidth enhancement factor further, the data collected for these five lasers is summarized in table 1. From this table it is seen that

as the height of the well barrier increases from 1.08 eV to 1.13 eV, together with a reduction in α parameter, there is also a large shift in the emission wavelength of the laser. This new wavelength of emission suggests that the uneven carrier distribution might have caused the output of the last three lasers to originate from a different quantum transition than that of the first two lasers, and this new transition has a much narrower spectral width.

If the conclusions in the last paragraph are correct, then the result presented in this section indicates that the depth of the well barrier and the choice of the right transition are important parameters to engineer lasers with narrow spectral widths.

V-4 Dependence of the Linewidth Enhancement Factor on the Output Power in InGaAsP Multi-quantum Well Semiconductor Lasers

In this section, the dependence of the linewidth enhancement factors on the output power of the lasers is presented. The data collected for the two lasers, S1-591 and S1-592, are presented in the next two figures. These two lasers were chosen because the band gaps of their quantum wells bracket the range covered by these five lasers.

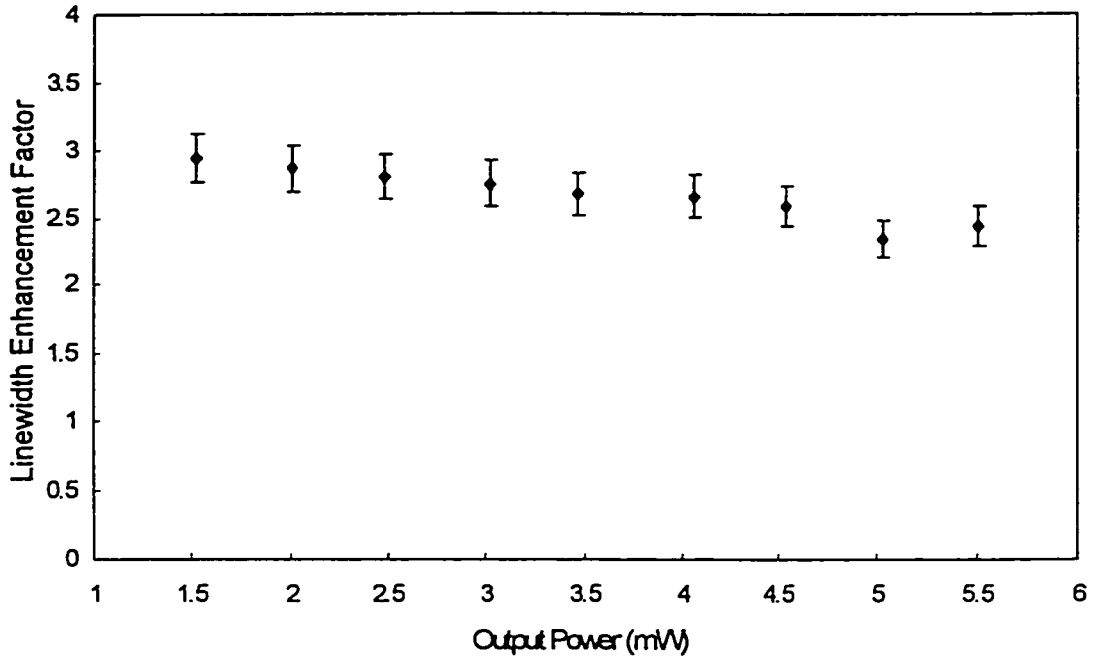

Figure 26: Linewidth enhancement factors versus output power for S1-592.

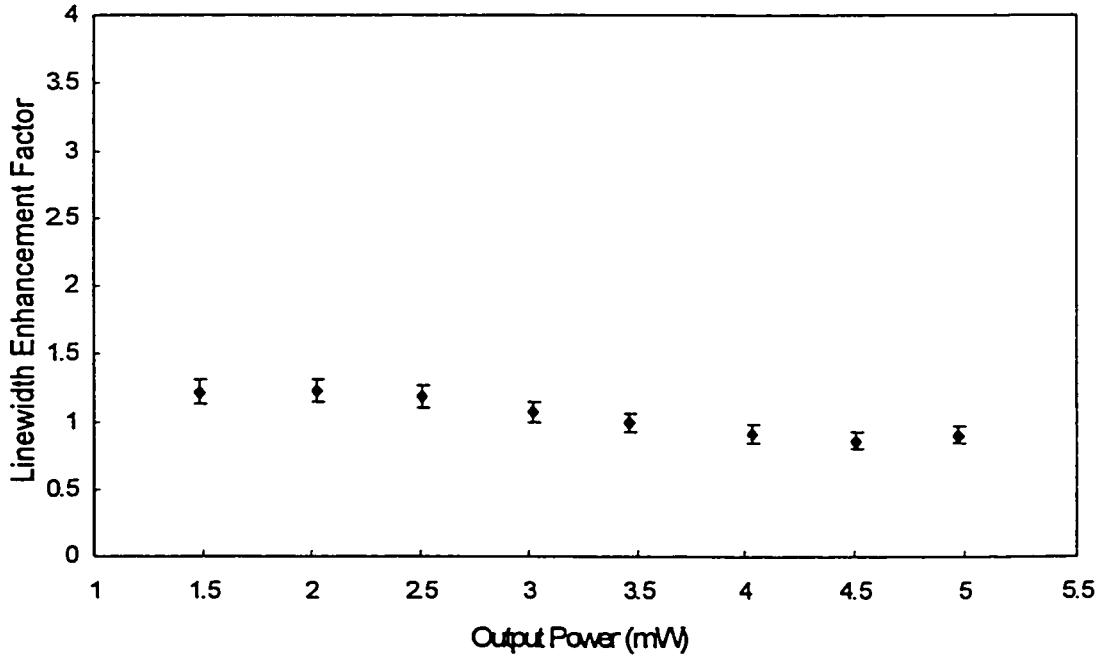

Figure 27: Linewidth enhancement factors versus output power for S1-591.

For both lasers, the linewidth enhancement factor of the mode that oscillates nearest to the gain peak was obtained as the output power was increased in 0.5 mW steps. This procedure was carried out until the side modes, which were originally suppressed by the SXC mirror, began to grow in intensity. For S1-592, the maximum power achieved before this happened was 5.5 mW, and for S1-591 the maximum power was 5 mW.

The data presented in Figs. 26 and 27 show that as the output power of the lasers increase, there is a very slight decrease in the linewidth enhancement factors.

Another study[65] performed on $1.55\mu m$ strained MQW distributed feedback lasers indicated that this slight downward trend in α parameter would be followed by a period of rapid increase. I did not observe this increase in my investigation. The reason for this is that my SXC mirror could not suppress the side modes at the high power range covered in this work so no measurement was performed there.

V-5 Summary

In this chapter, a brief background on quantum well lasers was presented with some emphasis on the differences between this class of lasers and the normal bulk lasers.

Having explained why quantum well lasers are important both fundamentally and technologically, a series of five InGaAsP MQW lasers were studied. It was found that the linewidth enhancement factors of these lasers depend on the wavelength of emission. In all five lasers, the linewidth enhancement factors attain their maximum

values around the gain peaks, and these values gently roll off as the wavelength of emission is tuned further and further away. It was also noted that, unlike the index-guided laser studied in chapter IV, as the wavelength of these lasers was tuned far enough from the gain peak the linewidth enhancement seems to increase again.

The dependence of the linewidth enhancement factors on the band gap of the barriers in the five quantum well lasers was also observed. It was found, on a coarse scale, that as the energy wells become deeper, the linewidth enhancement factor of the laser becomes smaller. It was also found that the five lasers could be divided into two groups. Within each group, where the groups were defined by the wavelength of emission, the linewidth enhancement factor increased slightly with the magnitude of the band gap of the barrier.

The dependence of the linewidth enhancement factors on the output power of the lasers was also studied in this chapter. Measurements were done on two lasers for this purpose. In both cases, it was found that as the output powers of the lasers increased the linewidth enhancement factors decreased. In fact, because the downward trend of the linewidth enhancement factors observed for these two lasers was slight and, because of the sizes of the error bars the linewidth enhancement factors were found to be essentially constant over the range of power studied.

VI- Conclusion

In this chapter, a summary of work done in this thesis is given, along with recommendation for future work.

VI-1 Summary of Work

In this thesis, a system has been developed for directly measuring the frequency-tuning characteristics in Fabry-Perot semiconductor lasers. From the frequency-tuning data, the linewidth enhancement factors of the lasers could be calculated. The system consists of a theoretical model of short external cavity (SXC) lasers and an experimental technique that realizes this model.

In the theoretical model, it was shown that by changing the length of the short external cavity the phase of the feedback light, from the SXC mirror, alters the resonant condition of the laser. This change in the resonant condition induces a shift in the frequency of emission of the laser. The thesis included a detailed derivation of a formula that related this shift in the frequency of emission to the linewidth enhancement factor of the laser.

An experimental set up was developed to make measurements of the laser frequency tuning with change in short external cavity length. An SXC laser module based on the flexure mount concept was constructed. The SXC system presented is inexpensive to construct. It is compact, sensitive, and stable. With the use of the flexure

mount, the alignment and the scanning of the external mirror is straightforward. Since near-IR InGaAsP/InP and AlGaAs/GaAs semiconductor diode lasers have become popular in many areas of research as sources of tunable, monochromatic radiation the flexure module presented here could be very useful in any application that requires lasers which operate on a single mode. In the experimental set up the tuning of the frequency of the laser was measured by tracking the displacement of the FPI mirrors. The experimental system was tested by making measurements on an index-guided and a quantum well laser. In both cases, the results obtained were within the expected range. The validity of this experimental technique was further confirmed by independent linewidth measurements on the same two lasers. The linewidth enhancement factors, obtained by this technique, were found to be quite insensitive to the magnitude of optical feedback from the SXC mirror. Once fully tested, the experimental system was used to study a series of five InGaAsP multi-quantum well lasers. These lasers have the same number of quantum wells, but the band gaps of the well barriers are different. Results of experiments showed that the linewidth enhancement factors of these lasers are wavelength-dependent and fairly power independent. It was also found, on a coarse scale, that as the band gap of the well barrier increases the magnitude of the linewidth enhancement factor decreases and that the five InGaAsP multi-quantum well lasers could be divided into two groups. Lasers with a barrier band gap of $\leq$ 1.08 eV and with an emission wavelength of 1.33 μm showed an α-factor of ≈ 3. Lasers with a barrier band gap of $\geq$ 1.13 eV and an emission wavelength between 1.27 - 1.29 μm showed an α-

factor of ≈ 1.2. Within each group, the linewidth enhancement factor increased slightly with increasing band gap of the barrier.

V-2 Recommendations for Future Work

There are many paths which could branch out from this thesis.

The linewidth enhancement factors of the quantum well lasers have been observed to be dependent on the wavelength of emission but the spectral range studied was quite limited. A natural extension is to expand the measurement to higher or lower wavelengths. This could be achieved by either positioning the SXC mirror closer to the back facet of the laser or by operating the laser at a different temperature.

In this study, the linewidth enhancement factors were found to be fairly independent of the output of the lasers. This observation may result from the fact that the range of power covered is limited by the performance of the SXC module. If a new experimental technique could be developed so that the laser could be operated at higher power without suffering from the noise from the side modes then it would seem useful to investigate further the effect of the output power on the α parameters.

The InGaAsP quantum well lasers studied in this thesis can be divided into two groups based on the wavelengths of emission. Within each group, the linewidth enhancement factors were found to increase slightly as the band gaps of the barriers increase. This result agrees with what Yariv [6] found in GaAs quantum well lasers. However, between these two groups the linewidth enhancement factor shows a sudden drop beyond a certain well depth. This observation is not clearly understood at this time,

and more work, on both experimental and theoretical sides, is required to reveal the cause of this phenomenon.

The most important goal of a study, like the one in this thesis, is to find out which laser parameter would affect the magnitude of the linewidth enhancement factor and bring about its reduction so that better lasers can be made. If lasers with different number of quantum wells could be found the method developed here could be used to find out if there is an optimal number of wells for minimum linewidth enhancement factors.

After completing this research, I am convinced that a thorough knowledge on linewidth enhancement factor is one of the key factors required to produce better performance lasers, and that the method developed here is a very useful means to further that knowledge. I hope that others will reach the same conclusion after reading this thesis.

References

[1] A. L. Schawlow and C. H. Townes, "Infrared and Optical Masers", *Phys. Rev.* **112**, pp. 1940-1949, 1958.

[2] M. Lax, "Classical Noise .V. Noise in Self-Sustained Oscillators", *Phys. Rev.* **160**, pp. 290-307, 1967.

[3] M. W. Fleming and A. Mooradian, "Fundamental line broadening of single mode (GaAl)As diode lasers", *Appl. Phys. Lett.*, **38**, pp. 511-513, 1981.

[4] T. G. Hodgkinson, chapter 6 in COHERENCE, AMPLIFICATION AND QUANTUM EFFECTS IN SEMICONDUCTOR LASERS, Y. Yamamoto Ed., John Wiley & Sons Inc., 1991.

[5] M. Ohtsu, and K. Nakagawa, chapter 5 COHERENCE, AMPLIFICATION AND QUANTUM EFFECTS IN SEMICONDUCTOR LASERS, Y. Yamamoto Ed., John Wiley & Sons Inc., 1991.

[6] B. Zhao, T. R. Chen, S. Wu, Y. H. Zhuan, Y. Yamaha, and A. Yariv, "Direct Measurement Of Linewidth Enhancement Factors In Quantum Well Lasers of different quantum well barrier heights.", *Appl. Phys. Lett.*, **62** , pp. 1591-1593, 1993.

[7] D. Kuksenkov, S. Feld, C.Wilmsen, and H. Temkin, "Linewidth and α-factor in AlGaAs/GaAs vertical cavity surface emitting lasers.", *Appl. Phys. Lett*, **66** , pp. 277-279, 1995.

[8] G. Hunzinker, W. Knop, P. Unger, and C. Harder, " Gain, Refractive Index, Linewidth Enhancement Factor from Spontaneous Emission of Strained GaInP Quantum-Well Lasers.", *IEEE J. Quantum. Electron.*, **QE-31**, pp. 643- 646, 1995.

[9] L. Olofsson, and T. G. Brown, "On the linewidth enhancement factors in semiconductor lasers" *App.l Phys. Lett.*, **57** , pp. 2773-2775, 1990.

[10] C.H. Henry, "Theory of the linewidth of semiconductor lasers", *IEEE J.Quantum Electron.*, **QE-18**, pp. 259-264, 1982.

[11] J. Ehrhardt, A. Villeneuve, G. I. Stegeman, H. Nakajima, J. Landreau, and A. Ougazzaden, "Interferometric Measurement of the Linewidth Enhancement Factor of a 1.55μm Strained Multiquantum-Well InGaAs/InGaAsP Amplifier.", *IEEE Photon. Technol. Lett.*, **4**, No. 12, pp. 1335-1338, 1992.

[12] K. Iiyama, K. Hayashi, and Y. Ida, "Simple method for measuring the linewidth enhancement factor of semiconductor lasers by optical injection locking.", *Opt. Lett.*, **17**, No. 16, pp. 1128-1130, 1992.

[13] U. Kruger and K. Kruger, "Simultaneous Measurement of the Linewidth, Linewidth Enhancement Factor α, and FM and AM Response of a Semiconductor Laser.", *IEEE J. Light. Tech.*, **13**, No. 4, pp. 592-597, 1995.

[14] S. Wang, and R. L. Hartman, "Measurements of dynamic linewidth enhancement factor and damping rate for distributed feedback lasers.", *SPIE* **1788**, "Sources and Detectors for Fiber Communications." pp. 89-100, 1992.

[15] K. Wada, M. Kitamura, Y. Akage, and Y. Cho, "Intensity and phase correlation method for determining the linewidth enhancement factor of semiconductor lasers.", *Optics Communication*, **110**, pp. 345-350, 1994.

[16] C. S. Chang, S. L. Chuang, J. R. Minch, Wei-chiao W. Fang, Y. K. Chen, and T. Tanbun-Ek, "Amplified Spontaneous Emission Spectroscopy in Strained Quantum-Well Lasers.", *IEEE J. Sel. Top. in Quantum. Electron.*, **4**, pp. 1100-1107, 1995.

[17] R. Hui, A. Mecozzi, A. D'Ottavi, and P. Spano, "Novel measurement technique of α factor in DFB semiconductor lasers by injection locking.", *Electron. Lett.*, **26**, pp. 997-998, 1990.

[18] C. H. Henry, R. Logan, and K. Bertness, "Spectral dependence of the change in refractive index due to carrier injection in GaAs lasers.", *J. Appl. Phys.*, **51**, pp. 3042-3050, 1980.

[19] M. Kesler and C. Harder, "Spontaneous emission and gain in GaAlAs quantum well lasers", *IEEE J. Quantum. Electron.*, **27**, pp. 1812-1816, 1991.

[20] P. Blood, A. I. Kucharska, J. P. Jacobs, and K. Griffiths, "Measurement and calculation of spontaneous recombination current and optical gain in GaAs-AlGaAs quantum-well structures.", *J. Appl. Phys.*, **70**, pp. 1144-1156, 1991.

[21] B. F. Ventrudo, and D. T. Cassidy, "Operating Characteristics of a Tunable Diode Laser Absorption Spectrometer using Short External Cavity and DFB Laser Diodes", *Appl. Opt.*, **29**, pp. 5007-5013, 1990.

[22] Shyh Wang, chapter 6 in FUNDAMENTALS OF SEMICONDUCTOR THEORY AND DEVICE PHYSICS, Prentice Hall, 1989.

[23] Shyh Wang, chapter 8 in FUNDAMENTALS OF SEMICONDUCTOR THEORY AND DEVICE PHYSICS, Prentice Hall, 1989.

[24] J. P. Van Der Ziel, and R. L. Mikuliak, "Single-Mode Operation of 1.3 μm InGaAsP/InP Buried Crescent Lasers Using a Short External Optical Cavity", *IEEE J. Quantum. Electron.*, **QE-20**, pp. 223-229, 1984.

[25] H. Kakiuchida, and J. Ohtsubo, "Characteristics of a Semiconductor Laser with External Feedback", *IEEE J. Quantum. Electron.*, **QE-30**, No 9, pp. 2087-2097, 1994.

[26] K. Petermann, "External Optical Feedback Phenomena in Semiconductor Lasers", *SPIE* **2450**, pp. 121-129, 1995, and references therein.

[27] L. J. Bonnell, and D. T. Cassidy, "Alignment Tolerances of Short External Cavity InGaAsP Diode Lasers for use as Tunable Single Mode Sources.", *Appl. Opt.*, **28**, pp. 4622-4628, 1989.

[28] T. Verdeyen, LASER ELECTRONICS, Prentice Hall, 2nd edition, 1989.

[29] B. E. A. Saleh, and M. C. Teich, FUNDAMENTAL OF PHOTONICS, Wiley-Interscience, 1991.

[30] K. Petermann, LASER DIODE MODULATION AND NOISE, Kluwer Academic Publishers, 1991.

[31] Shane Woodside, LINEWIDTH OF SHORT EXTERNAL CAVITY SEMICONDUCTOR LASERS, M.Eng. Thesis, Engineering Physics Department, McMaster University, 1992.

[32] A. Nguyen and D. T. Cassidy, "Flexure-mounted external cavity for single-mode operation of semiconductor diode lasers.", *Rev. Sci. Instrum.*, **66**, pp. 4458-4460, 1995.

[33] D. K. Kreid, "Versatile Flexure Mount for Precise Positioning of Optical Elements", *Appl. Opt.*, **13**, pp. 737-738 , 1974.

[34] COHERENCE, AMPLIFICATION, AND QUANTUM EFFECTS IN SEMICONDUCTOR LASERS, Y. Yamamoto Ed., John Wiley & Sons Inc., 1991.

[35] T. Kanada and K. Nawata, "Single-Mode Operation of a Modulated Laser Diode with a Short External Cavity", *Opt. Comm.*, **31**, pp. 81-84, 1979.

[36] C. Lin, C. A. Burrus, and L. A. Golden, "Characteristics of Single Longitudinal Mode Selection in Short-Coupled-Cavity (SCC) Injections Lasers", *IEEE/OSA J. Lightwave Technol.*, **LT2**, pp. 544-549, 1984.

[37] G. P. Agrawal, "Generalized rate equations and modulation characteristics of external-cavity semiconductor lasers", *J. Appl. Phys.* **56**, pp. 3110-3115, 1984.

[38] M. R. Mathews, K. H. Cameron, R. Wyatt, and W. J. Devlin,"Packaged Frequency-Stabled Tunable 20 kHz Linewidth 1.5 μm InGaAsP External-Cavity Laser", *Electron. Lett.*, **21**, pp. 113-115, 1985.

[39] G. P. Agrawal and N. K. Dutta, LONG WAVELENGTH SEMICONDUCTOR LASERS, Nostrand Reinhold, New York, 1986.

[40] C. E. Wieman and L. Hollberg, "Using Diode Lasers for Atomic Physics", *Rev. Sci. Instrum.*, **62**, pp. 1-20, 1991.

[41] J. Buus, SINGLE FREQUENCY SEMICONDUCTOR LASERS, *SPIE Optical Engineering*, Bellingham, 1991.

[42] P. R. Bevington, DATA REDUCTION AND ERROR ANALYSIS FOR THE PHYSICAL SCIENCES, McGraw-Hill Book company, 1969.

[43] N. K. Dutta, N. A. Olson, H. K. Temkin, R. A. Logan, and T. Tanbun-Ek, "Linewidth Enhancement Factor and High Temperature Performance of 1.48 μm Strained InGaAs-InGaAsP Multiquantum Well Lasers.", IEEE J. Quantum. Electron., vol. 27, No. 3, pp. 678-680, 1991.

[44] L. F. Tiemeijer, P. J. A. Thijs, P. J. de Waard, J. J. M. Binsma, and T. v. Dongen,, "Dependence of polarization, gain, linewidth enhancement factor, and K factor on the sign of the strain of InGaAs/InP strained-layer multiquantum well lasers.", Appl. Phys. Lett. Vol. 58, No. 24, pp. 2738-2740, 1991.

[45] N. K. Dutta, H. Temkin, T. Tanbun-Ek, and R. Logan, "Linewidth Enhancement factor for InGaAs/InP strained quantum well lasers", Appl. Phys. Lett, vol. 57, No 14, pp. 1390-1391, 1990

[46] J. F. Hazell, THE EFFECTS OF VARYING ACTIVE REGION BARRIER COMPOSITION ON THE OUTPUT CHARACTERISTICS OF 1.3 μm InGaAsP STRAINED LAYER MQW LASERS, M. Eng. Thesis, McMaster University, 1995.

[47] B. Zhao, T. R. Chen, and A. Yariv, "A Comparison of Amplitude-Phase Coupling and Linewidth Enhancement in Semiconductor Quantum-Well and Bulk Lasers", *IEEE J. Quantum. Electron.*, **29**, pp. 1027-1030, 1993.

[48] K. Iiyama, K. Hayashi, Y. Ida, and S. Tabata, "Delayed Self-Homodyne Method Using Solitary Monomode Fibre for Laser Linewidth Measurements", *Electron.Lett.*, **25**, pp. 1589-1590, 1989.

[49] E. Patzak, H. Olesen, A. Sugimura, S. Saito, and T. Mukai, "Spectral Linewidth Reduction in Semiconductor Lasers by an External Cavity with Weak Optical Feedback", *Electron.Lett.*, **19**, pp. 938-940, 1983.

[50] G. P. Agrawal, "Line Narrowing in a Single-Mode Injection Laser due to External Optical Feedback", *IEEE J. Quantum. Electron.*, **QE-20**, pp. 468-471, 1984.

[51] N. A. Olsson, C. H. Henry, R. F. Kazarinov, H. J. Lee, B. H. Johnson, and K. J. Orlowsky, "Narrow linewidth 1.5μm semiconductor laser with a resonant optical reflector", *Appl. Phys. Lett.*, **51**, pp. 1141-1142, 1987.

[52] C. H. Shin and M. Ohtsu, "Stable semiconductor laser with a 7-Hz linewidth by an optical-electrical double-feedback technique", *opt. Lett.*, **15**, pp. 1455-1457, 1990.

[53] L. Li, "Theory for the Spectral Linewidth of Passive-Coupled Cavity", *IEEE J. Quantum. Electron.*, **QE-26**, pp. 3-5, 1990.

[54] H. Sun, S. Menhart, and A. Adams, "Calculation of spectral linewidth reduction of external-cavity strong-feedback semiconductor lasers", *Appl. Opt.*, **33**, pp. 4771-4775, 1994.

[55] R. G. Hunsperger, chapter 16 in INTERGRATED OPTICS: THEORY AND TECHNOLOGY, third edition, Springer-Verlag, 1991.

[56] M. A. Morrison, chapter 7 in UNDERSTANDING QUANTUM PHYSICS, Prentice Hall Inc., 1990.

[57] Peter S. Zory, Jr., QUANTUM WELL LASERS, Accademic Press Inc., 1993.

[58] M. G. Burt, "Linewidth Enhancement Factor for Quantum-WellLasers", *Electron. Lett.*, **20**, pp. 27-28, 1984.

[59] Y. Anakawa and A. Yariv, "Theory of Gain, Modulation Response, and Spectral Linewidth in AlGaAs Quantum Well Lasers", *IEEE J. Quantum. Electron.*, **QE-21**, pp. 1666-1674, 1985.

[60] T. Ohtoshi and N. Chinone, "Linewidth Enhancement Factor in Strained Quantum Well Lasers", *IEEE Photonics Technol. Lett.*, **1**, pp. 117-118, 1989.

[61] L. Olofsson and T. G. Brown, "On the linewidth enhancement factor in semiconductor lasers", *Appl. Phys. Lett.*, **57**, pp. 2773-2775, 1990.

[62] S. H. Cho, C. C. Lu, M. Hovinen, K.nam, V. Vusirikala, J. H. Song, F. G. Johnson, D. Stone, and M. Dagenais, "Dependence of the Linewidth Enhancement Factor on the Number of Compressively Strained Quantum Well in Lasers", *IEEE Photonics Technol. Lett.*, **9**, pp. 1081-1083, 1997.

[63] J. F. Hazell, J. G. Simmons, J. D. Evans, and C. Blaauw, "The Effect of Varying Barrier Height on the Operational Characteristics of 1.3-μm Strained-Layer MQW Lasers", *IEEE J. Quantum. Electron.*, **QE-34**, pp. 2358-2363, 1998.

[64] M. J. Hamp, D. T. Cassidy, B. J. Robinson, Q. C. Zhao, D. A. Thompson, and M. Davies, "Effect of Barrier Height on the Uneven Carrier Distribution in Asymmetric Multiple-Quantum-Well InGaAsP Lasers", *IEEE Photonics Technol. Lett.*, **10**, pp. 1380-1382, 1998.

[65] H. Nakajima and J. C. Bouley, "Observation of Power Dependent Linewidth Enhancement Factor in 1.55 μm Strained Quantum Well Lasers", *Electron. Lett.*, **27**, pp. 1840-1841, 1991.